

Chromosomal rearrangements as a source of local adaptation in island *Drosophila*

Brandon A. Turner^{*1}, Theresa R. Miorin^{*2}, Nicholas B. Stewart³,
Robert W. Reid¹, Cathy C. Moore¹ and Rebekah L. Rogers¹

1. Department of Bioinformatics and Genomics, University of North Carolina, Charlotte NC
2. Dept of Genetics, University of Georgia, Athens, GA
3. Dept of Biology, Ft. Hays State University, Hays, KS

*These authors contributed equally to this work.

Keywords: Structural variation, genetic novelty, local adaptation, habitat shifts

Introduction

The genetic response to shifting selective pressures remains one of the most fundamental questions in evolutionary theory. How does genetic variation appear and contribute to phenotypic changes during sudden or extreme shifts in habitat [1]? Among the potential genetic responders to selection, SNPs have received ready attention in theory and in empirical studies of differentiation. However, structural variants are often masked or ignored as these mutations are more difficult to identify and interpret in genetic sequence data [2–5]. This source of genetic variation deserves greater observation in the context of evolutionary change. Mutations that copy or shuffle pieces of DNA within the genome can join new linkage groups, alter gene expression patterns, or create new gene sequences where none existed before [6–9]. As such we hypothesize they are a source of innovation that likely to produce cellular changes when they are necessary during habitat shifts. We wish to discern whether these “hopeful monsters” among genes might lead to adaptive success in new environments.

Among the many fundamental questions facing local adaptation, the role of new mutation and standing variation is debated [10–12]. To what extent is adaptation limited by the span of standing variation in populations? How long might it take to acquire new mutations when selective pressures shift? Over time, due to factors such as allopatry, genetic drift, and reproductive isolation, populations can begin to diverge [13]. Selection on adaptive mutations allow these populations and species to become better suited to their environments. How these adaptive mutations come about is still a question that remains.

The tempo and magnitude of evolutionary change depend on the available substrate of variation, as well as evolutionary forces. Standing variation may fix rapidly in response to environmental shifts [10], but the spectrum of available variation will be limited by population genetic forces [11]. Mutations with fitness impacts greater than the nearly neutral threshold are expected to be weeded out of populations quickly [14, 15]. Even among neutral variation, segregating variation will depend on mutation rates and population sizes [16]. Meanwhile long wait times for new mutations may place bounds on how quickly genomes can adapt through new mutations [17]. If mechanisms exist generate the supply of new mutations, it may be possible to generate variation quickly during habitat shifts. Discerning how new mutations appear in populations and spread during habitat changes is imperative to evaluate the genetic response to rapid or drastic shifts in selective pressures.

Recent technological innovation has allowed us to identify such variation in high throughput large scale genome sequencing panels [18–21], opening doors to study evolutionary impact in new organisms or systems beyond standard models [22]. We are able to discover how these mutations contribute to population variation and how their allele frequencies shift in differing environmental contexts. One evolutionary system that has experienced such habitat shifts is the *D. yakuba*-*D. santomea* species complex. *D. yakuba* contains a large number of chromosomal rearrangements [23–25] that have shown evidence of being linked to the creation of de novo exons, providing a source of new gene formation [26].

D. yakuba and *D. santomea* are two sister species of *Drosophila* that have both adapted to the island habitats of São Tomè in the past 500,000 years [27]. These two species inhabit separate elevations on the island, with *D. santomea* living in higher elevations and absent in the lower regions of the island where *D. yakuba* is abundant [28]. They do have a contact zone at moderate altitude, however, where hybrids can occur [29]. The two species likely diverged

in allopatry, and during this time partial sexual and post-zygotic isolation evolved [29]. This is reflective of a second invasion of *D. yakuba* [28, 30, 31], which has not yet completely diverged from the mainland population of *D. yakuba*, but has not had the time to diverge compared to established populations like *D. santomea* [27]. This species complex provides a unique opportunity to study and understand genetic variation between two closely related species on a single island.

This complex is ideal for population genetics of local adaptation as it has invaded far enough in the past that phenotypic and genetic differentiation can occur [29, 32]. However, it is not yet so long in the past that population genetic signals are obscured by new mutations and left to be seen only in species divergence [33]. It further benefits from a known ancestral mainland population that is well characterized for structural variation [20, 34]. To build on these strengths of the *D. yakuba-D. santomea* system, we have generated population genetic panels for *D. yakuba* and *D. santomea* on São Tomè with paired end Illumina and PacBio HiFi sequencing. We pair these data with gene expression analysis to identify cases where structural variants alter expression or create new genes.

This comprehensive portrait of structural variation in local adaptation on São Tomè can serve as the basis for future insights on evolutionary responses in shifting selective pressures. By learning how chromosomal rearrangements result in phenotypic changes we can better understand how rapid evolution can reshape populations in nature.

Results

Rearrangements role in population differentiation

We wished to determine whether chromosomal rearrangements serve as new sources of genetic variation during habitat shifts. To assay this source of genetic novelty during local adaptation, we identified rearrangements in populations of *D. santomea* and *D. yakuba* on the island of São Tomè. Mainland *D. yakuba* are the known ancestral population to both *D. santomea* and the island *D. yakuba* on São Tomè [35]. These two waves of island invasion offer independent cases of local adaptation from the same mainland population. By surveying the differences in island environments we can determine how chromosomal rearrangements serve as agents of local adaptation.

The metapopulation consists of three sub-populations, the island *D. santomea* and *D. yakuba*, as well as the ancestral source of variation, mainland *D. yakuba*. We used Illumina paired-end reads to identify chromosomal rearrangements and validated genotypes with PacBio HiFi sequences. We identify find 3,412 rearrangements associated with 19 strains of mainland *D. yakuba*, 7,093 with 35 strains of island *D. yakuba*, and 7,796 with 42 strains of *D. santomea* out 16,480 total rearrangements for the meta-population (Figure S1, S2). The number of rearrangements found per strain varies from 82 to 875 total rearrangements in a strain (Table 1). Using PacBio long read data we show that the confirmation rate of rearrangements is 100% when using a combination of four alignment methods, minimap2 [36], Sniffles [37], and PacBio’s pbsv [38]. We find 6,588 genes within 5kb of the rearrangement’s breakpoints (Table 2).

For each rearrangement we calculate the allele frequency for the metapopulation, as well

as the frequency in each subpopulation. These frequencies are corrected residual heterozygosity created by inbreeding resistance at inversions similar to prior work [39]. Calculating the differences in the populations at rearrangements we can infer what changes have accumulated in the *D. santomea* since their separation from the mainland *D. yakuba*. We identify variants that are outliers compared with genome wide expectations, that have putatively spread through island populations due to selection. The three site frequency spectra (SFS) when projected down to the same sample size of $n=19$ (Figures 1a, 1b, 1c) show, most of the rearrangements at low frequency, as expected. We observe increases at high frequency, with 20.7% of the projected mutations with a frequency of 18/19 or higher. This increase at high frequency in the SFS could signal that rearrangements are disproportionately responsible for rapid adaptation when a population is suddenly introduced to a new environment. The distribution of the SFS for *D. santomea* rearrangements is statistically different (Kolmogorov-Smirnov, $D = 0.65$, $P = 0.00027$) than that of SNPs in *D. santomea*, implying that allele frequency of rearrangements behave differently than that of the clock-like SNPs in the population. This is also true for the island *D. yakuba* (Kolmogorov-Smirnov, $D = 0.65$, $P = 0.00027$) and the mainland *D. yakuba* (Kolmogorov-Smirnov, $D = 0.7$, $P = 5.6 \times 10^{-5}$).

The sex chromosomes show more dynamic occurrence of rearrangements on the sex chromosomes. The autosomes averaged 1,684 mutations each (s.d = 251.68), whereas the X chromosome has 2,814.

Transposable elements and structural variation

Transposable elements (TEs) facilitate formation of chromosomal rearrangements. TE insertions can result in duplications of nearby sequence and also cause ectopic recombination [40]. Using BLAST, we compare the rearrangement breakpoints clustered across strains against the RepBase database [41]. We find that 13,763 of 16,480 (83.5%) rearrangements are associated with TEs. Only 5.5% of the reference genome is composed of TEs [42]. Hence, we observe that rearrangements are heavily linked with transposable elements.

We see 9,152 out of 16,480 (55.5%) associated with TE insertions and 4,611 of the 16,480 (28.0%) rearrangements show evidence that transposable elements are facilitating local adaptation via ectopic recombination. The remaining 2,717 of 16,480 (16.5%) rearrangements show no association with transposable elements.

Rearrangements are enriched near the centromeres where recombination suppression allows detrimental variation to accumulate (Figure S3). Novel TE insertions show the majority of high frequency variants in island environments (Figure S4 and Figure S5; Table 3). Genome wide there are more new TE insertions than cases of ectopic recombination (Figure S6, S7, S8, S9), with the proportion of ectopic recombination sites being 3116/16,480 (18.9%). Near the centromeres (within 3Mb) we see the proportion of rearrangements facilitating ectopic recombination rise to 1,990/3,562 (55.9%). This implies that rearrangements near the centromere are disproportionately responsible for facilitating ectopic recombination.

Each TE family has a different history, and previous work has shown that when certain TE families are enriched they can affect transcriptional regulation of stress response genes [43]. Here we show that the top 10 TE families are associated with 14345/18374 (78.1%) of rearrangements in the metapopulation (Figure S10). The proportion of TE fam-

ily representation is similar in *D. santomea* where the same top 10 account for 5741/6659 (86.2%), as well as 5301/5939 (89.3%) in *D. yakuba* (Figure S11). These proportions show a significant difference considering variants with significant population differentiation where we see 446/533 (83.7%) in *D. santomea* are associated with the top 10 out of 60 TE families represented ($\chi^2 = 333.58$, $P = 1.455 \times 10^{-6}$) and in *D. yakuba* 314/381 (82.4) ($\chi^2 = 316.84$, $P = 2.461 \times 10^{-5}$) and minor elements are over represented. This implies that some TE families may be more likely to induce adaptive variation and contribute to population differentiation more than expected based on incidence rates.

The way that species react to sudden changes in environment can result in a rapid burst of new variation that creates genetic novelty in the genome [1]. While most will be neutral or detrimental [14, 15], these bursts could offer variation that may fortuitously help species like *D. santomea* rapidly adapted to their new environment on São Tomè. To determine the role that rearrangements have in this adaptation we compare both the *D. santomea* and island *D. yakuba* to the mainland *D. yakuba*. With the SFS showing that the TEs are responsible for the high frequency variants (Figure S4), TEs are playing a role in this system (Kolmogorov-Smirnov, $D = 0.65$, $P = 0.00027$) [44].

Local adaptation and Structural variation

We identified rearrangements with strong differentiation between island populations and ancestral mainland *D. yakuba*. In local adaptation, prior simulations suggest that when the ancestral population is known, Δp , the change in allele frequencies, may incorporate additional information about evolutionary response to selection [45]. When populations have had sufficient time for local adaptation, Δp may in fact offer greater power to detect shifts in selection than even F_{ST} [45]. This statistic reflects a directionality, positive or negative, that captures allele frequency changes [45].

To show the differences between the groups we use the population differentiation statistics Δp and F_{ST} . We observe differences that have accumulated in *D. santomea*, with peaks in Δp that are seen in *D. santomea* (Figure 2a) but not in the island *D. yakuba* (Figure 2c). By comparing the distribution to neutral SNPs, from bp 8-30 at first introns [46], in the genome we can determine the threshold of Δp that should be used to determine if a mutations differentiation is beyond expectations for the genome as a whole.

We observe 468 rearrangements with significant differentiation in *D. santomea*, and 383 mutations with significant differentiation in *D. yakuba*. Some 41 rearrangements with signals of genetic differentiation are shared among the two locally adapted species, suggesting that identical genetic solutions to survival on São Tomè is exceptionally rare. The X chromosome has a notably more dynamic differentiation across populations compared to autosomes for the distribution of Δp when compared with the autosomes in both the *D. santomea* (Kolmogorov-Smirnov, $D = 0.28$, $P = 1.603 \times 10^{-8}$) and island *D. yakuba* (Kolmogorov-Smirnov, $D = 0.14$, $P < 2.2 \times 10^{-16}$) populations. We also show that on most of the autosomes there is a more positive skew in the Δp for the *D. santomea* than the island *D. yakuba*, consistent with the earlier invasion time for *D. santomea* and extended timeline of local adaptation [27, 31]. On the sex chromosome however Δp is shown to be more dynamic in both the island *D. yakuba* and *D. santomea* when compared to the Δp values of the autosomes. The excess of mutations on the sex chromosomes supports other work that has

shown higher rates of rearrangements out of the X [47] and the outsized role of the X in speciation [33, 48]. F_{ST} can identify population differentiation even when allele frequencies are low, and offers a secondary assessment of whether genome structure changes are associated with population differentiation. We observe 180 rearrangements with high F_{ST} . Together, these metrics each show that structural variants show strong differentiation between island populations and the mainland (Figure S12, S13).

Transposable element families each have different histories and recent activity levels, and by looking at which families are associated with rearrangements more often we can ascertain whether specific families are disproportionately associated with rearrangements that have Δp outside of the 95% C.I. We show that while 446/533 (83.7%) number of significantly differentiated rearrangements are associated with just the top 10 out of 60 TE families represented (Figure S11), these same TE families are represented at roughly same rate in rearrangements that did not have significant Δp (Figure S10, implying that there is likely no specific TE family is directly responsible for adaptive change.

Gene expression changes and gene fusions role in significant rearrangements

Rearrangements often produce changes in gene expression [9]. We use CuffDiff [49] to determine whether the genes that are within 5kb of a rearrangement show statistically significant gene expression. We observe 3008/16480 (18.3%) rearrangements that are within 5kb of regions that show statistically significant (Fisher’s combined $p \leq 0.05$) changes in gene expression in at least one tissue for these regions. To determine whether chromosomal rearrangements are causative agents of gene expression changes, we can determine if these are disproportionate to what we would expect by chance alone using a bootstrap approach.

In *D. santomea* we show 2,032 unique genes that are differentially expressed among strains with rearrangements, and these genes are expressed in a total of 4,572/16,480 (27.7%) across the four tissues sampled (testes, ovaries, male soma, female soma). Across tissues, we observe 1,813/16,480 (11.0%) are expressed in the testes, 1,361/16,480 (8.3%) in the ovaries, 1,205/16,480 (7.3%) in the male soma, and 193/16,480 (1.2%) in the female soma. Similarly, when looking at the mainland *D. yakuba* we see a total of 902 unique genes that are differentially expressed in strains with rearrangements (Figure S14, S15). These genes are expressed in a total of 1,947/16,480 (11.8%) across the four tissues. Of these genes 744/16,480 (4.5%) are seen in the testes, 563/16,480(3.4%) in the ovaries, 516/16,480 (3.1%) in the male soma, and 124/16,480 (0.8%) in the female soma. Lastly in the island *D. yakuba* we see 1,282 unique genes that are differentially expressed, and these genes are expressed in a total of 2,863 across the four tissues. which 1,041/2,863 (36.4%) are in the testes, 912/2,863 (31.9%) in the ovaries, 770/2,863 (26.8%) in the male soma, and 140/2,863 (4.9%) in the female soma.

We used Tophat fusion search [50] to find fusions transcripts indicative of chimeric gene formation. We identify only 15 rearrangements that are associated with gene fusions suggesting chimeric gene formation. These fusions are not associated with signatures of local adaptation, in spite of previous work identifying signatures of selection on chimeric genes in *Drosophila* [5, 21].

In *D. santomea*, of the 145/244 (59.4%) mutations that show significant population differentiation and significant gene expression changes, and 6 associated with fusion transcripts (Figure 3). We see in the island *D. yakuba* that 99/217 (45.6%) rearrangements show significant population differentiation and display changes gene expression (Figure 3, Figure S15). Rearrangements with changes in gene expression are skewed toward increases in frequency for both island *D. santomea* (Kolmogorov-Smirnov, $D = 0.17$, $P = 0.0047$) (Figure 3) and island *D. yakuba* (Kolmogorov-Smirnov, $D = 0.19$, $P = 2.2 \times 10^{-16}$) (Figure S15). The majority of genes that showed significant expression changes in both populations on São Tomè are shown to have at least one breakpoint associated with a TE as well, lending to the idea that TEs are facilitating adaptation via a rapid burst of new insertions associated with effects on gene expression.

New mutations versus standing variation in local adaptation

During habitat shifts, adaptation can come from new mutations that occur once the population is moved to a new environment [51], or from standing variation which existed in the population before the shift [10]. While the majority of mutations will be either neutral or detrimental, there will be occasions where a new phenotype can proliferate through a population due to the advantage it confers. Standing variation in the genome existing at the time of a habitat shift offers a source of mutations readily available for a population to exploit to their advantage, rather than needing to create novel variation through mutation [20].

By comparing the two modes of evolution from standing variation and new mutations we can further understand how each play a role in adaptation, especially when a population experiences a sudden change in habitat. We observe many instances where a mutation in *D. yakuba* that is absent in the mainland *D. yakuba* has moved to a moderate frequency. We observe in *D. santomea* that 155/244 (63.5%) rearrangements have Δp outside of the 95 percent CI and are new mutations, with the remaining 89/244 (36.5%) being from standing variation. Similarly for the island *D. yakuba* flies we see 157/217 (72.4%) rearrangements are new mutations, and 60/217 (27.6%) are from standing variation. The mean of the significant Δp points is 0.1551 for new mutations and 0.2193 for the standing variation in *D. santomea*, and 0.1622 and 0.2430 respectively in the island *D. yakuba* (Figure 5). While there are a total of more new mutations than standing variation, they appear to trend at a lower allele frequency than standing variation (Figure 6, S16, S17). These results are consistent with standing variation having had more time to spread through the population.

Chromosomal Rearrangements are associated with UV resistance genes

D. santomea reside at a higher elevation than both the island and mainland *D. yakuba*, exposing them to greater UV stress [28]. Despite this known selective pressure for *Drosophila*, they are actually paler than ancestral *D. yakuba* flies [35]. The phenotypic differences in *D. santomea* are a long-standing open question for how these pale flies survive in environments where other species are selected for melanistic phenotypes [52, 53].

Among all adaptive rearrangements, three of the most dynamic candidate regions are at the locus of UV repair genes: *Parp* and UV tolerance gene *Victoria*, and *spell1* (Figure

4. High altitude *D. santomea* experience greater UV exposure, yet with the non-melanistic phenotypes it remains a mystery how *Drosophila* might tolerate such environments. We see four rearrangements within 5kb of *Parp*, with one variant showing an allele frequency of 0.317, a Δp p of 0.268, and an F_{ST} of 0.071. We can also see a reduction in Tajima's D to a local minima of -1.89 (Figure 4) signaling strong positive selection. A rearrangement within 5kb of *Victoria* has a frequency of 0.419, Δp p of 0.38, and F_{ST} of 0.125 (Figure 4). Nine other rearrangements are within 5kb of *Victoria*, however they are singletons in one of the three sub-populations. Tajima's D and π are positive in the region (Figure 4), but previous literature has shown soft sweeps may cause increases in Tajima's D due to an excess of moderate frequency alleles [54]. Notably, the one mainland *D. yakuba* strain that is associated with the *Victoria* ortholog rearrangement is the same sole strain found in the *Parp* ortholog's rearrangement.

We see another instance of a rearrangement possibly affecting DNA repair in the case of *spell1* (Figure 4). *spell1* is a MutS homolog that promotes the correction of DNA mismatches during replication, recombination, and repair [55]. We observe 4 independent rearrangements that are 2-6kb downstream of *spell1* that all show strong differentiation. Across these 4 mutations Δp lies outside of the 95% C.I, ranging from 0.078 to 0.39. We also show that both rearrangement breakpoints are associated with TEs in RepBase, suggesting formation through ectopic recombination. We see significant expression changes for both *Parp* and *spell1*, but not *Victoria*.

These independent adaptive rearrangements at three different loci associated with UV repair suggest strong selective pressures in *D. santomea*. Here, analysis of chromosomal rearrangements in local adaptation can reveal genetic variation that has been missed in SNP-based surveys of *D. yakuba* and *D. santomea*. Surveying this long neglected source of genetic variation reveals answers to long standing mysteries regarding the genetic basis of UV tolerance at high altitude.

Rearrangements associated with other biological functions

While UV associated variation answers long standing questions regarding the genetic basis of local adaptation, population genetic screens also have the power to identify adaptive changes without bias toward any single functional category. In these screens for alleles with high divergence across populations, we observe adaptive rearrangements whose precise cellular and phenotypic impacts in island environments remain somewhat less clear. We also observe structural variation at genes with other functions such as rearrangement near genes that are orthologous to *NijA*, another stress and immune response gene [56] with an allele frequency of 0.671 in *D. santomea* and 0.884 in *D. yakuba*. We also see *pnut*, a gene whose proteins aid in cytokinesis [57] and other cellular organization which is seen at a frequency of 0.205 in *D. santomea* and 0.0 *D. yakuba* (Figure S18). We identify *NUCB1*, a gene related to stress and behavior in *Drosophila* [58] seen at a frequency of 0.585 in *D. santomea* and 0.974 in *D. yakuba*. We see a rearrangement at moderate frequency that is an ortholog to the gene *Smr*. *Smr* is a transcriptional corepressor that influences *Drosophila* developmental genes such as *Notch* and ecdysone signaling [59]. This rearrangement is found in 27/72 (0.361%) of *D. santomea* and 1/20 (0.05%) of mainland *D. yakuba*. This, like other cases, is one that shows a moderate allele frequency in the island *D. santomea*. We also show two cases (S19) that

have no genes within 10kb, where we see significant population differentiation ($\Delta p=0.4651$ and $\Delta p=0.3485$), as well as noticeable changes in the signatures of selection through drops in π and Tajima's D (Table S1).

Population genetic scans suggest that these rearrangement facilitates local adaptation through mechanisms that remain yet to be discovered. The rearrangement being at moderate frequency and related to the developmental processes in *Drosophila* could signal that rearrangements are responsible for adaptation through phenotypes that we have not yet understood.

Discussion

Structural variation responds to habitat changes

Three independent adaptive rearrangements at three different loci associated with UV repair suggest strong selective pressures in *D. santomea*. Here, analysis of chromosomal rearrangements in local adaptation can reveal genetic variation that has been missed in SNP-based surveys of *D. yakuba* and *D. santomea*. While high altitude flies often evolve melanistic phenotypes for protection, *D. santomea* is pale [35, 60]. Structural variation offers multiple genetic solutions for DNA integrity in the face of increased radiation [61]. Surveying this neglected source of genetic variation reveals answers to long standing mysteries regarding the genetic basis of UV tolerance at high altitude [60, 62]. Flies lacking the *spell1* gene suffer a highly in long runs of dinucleotide repeats after 10-12 fly generations [63]. MutS mutants are associated with greater sensitivity to DNA damage, including UV stress.

We also observe structural variation at genes with other functions such as rearrangement near genes that are orthologous to stress and immune response genes, cytokinesis, and stress and behavior among others. We also observe regions that have no genes within 10kb, yet show changes in the signatures of selection (Figure S18). We observe more extreme signals of local adaptation and differentiation from the mainland on the X chromosome compared with the autosomes. These impacts are consistent with larger amounts of repetitive sequences on the X chromosome. The *D. yakuba-D. santomea* species complex is known to interbreed, with partially sterile hybrids. The high levels of differentiation on the X chromosome are consistent with the large-X effect in speciation, where interactions among species that are partially reproductively isolated may be driving some part of sex-linked differences.

Many of the rearrangements we identify as targets of selection are found to alter gene expression, consistent with prior work [9], suggesting that these mutations create important changes in gene regulation that are causative agents of local adaptation. Without information about rearrangements, SNP-based studies [64] offer an incomplete account of the genetic changes between populations and the diverse solutions they offer to selective pressures. As technological advances continue, it is imperative that we continue to survey the impacts of these mutations and their phenotypic effects in evolutionary and biomedical genetics.

Genetic convergence is rare in adaptation to São Tomè

The *D. yakuba*-*D. santomea* species complex is an excellent model to study the genetic basis of habitat shifts as it offers two different species adapted to the same island: *D. santomea* at high altitude and *D. yakuba* in the lowlands [28]. The two species may also interbreed in nature, offering the opportunity for adaptation through allele-sharing [29,47,48,52]. However, in these two species we see few cases of identical mutations spreading in island environments (7.3%). In these environments we have shown that chromosomal rearrangements can serve as “hopeful monsters” of the genetic world. However, the specific monsters that are favored differ widely across populations.

Genome structure changes remain understudied in evolutionary genetics compared to single base pair changes. However, here, we have shown that these mutations can create dynamic changes in the genetic substrate available during adaptation during selective shifts. Studying genome structure changes in local adaptation and habitat invasion is essential to understand how genetic diversity facilitates phenotypic changes in nature. The ability to perform parallel analysis of these mutations in two independent cases of habitat invasion with a known ancestral population lends greater strength to evolutionary inference as rearrangements appear to be important players in evolutionary processes in nature.

Structural variation and transposable elements

Transposable elements are selfish DNA that proliferates within the genome even at the expense of the host organism. TEs often appear in bursts and can rapidly remodel multiple genes on short timescales. These mutations depart from the clock-like progression of mutations at SNPs, with boom-and-bust dynamics as cells engage in arms races to develop repressors that keep TE proliferation in check. In times of stress, TEs can activate and occasionally create variation that remodels gene expression under specific environmental conditions or developmental processes [65–67]. In this work we observe a significant proportion of new mutations that are created by transposable elements. New TE insertions appear in abundance, however ectopic recombination among distantly related TE copies is common as well. The majority of these mutations do not spread in island environments, and appear to be neutral or detrimental. However, a distinct subset appears to spread in populations as they adapt to new and changing environments.

Prior work in other systems such as plants have observed functional biases from different classes of TEs. Among all chromosomal rearrangements, no single TE class is enriched among variation that is targeted by natural selection, but rather reflects the relative abundance of TE classes that have modified DNA within the genome. This result implies that the selective impacts of TE-induced mutations are random, not biased to a specific TE type. Both island populations of *D. santomea* and *D. yakuba* show different sets of mutations serving as targets of selection, showing independent that TE induced rearrangement facilitates adaptive changes. DNA transposons and retrotransposons across multiple TE families are represented, implying multiple TE activation events rather than a single activation of only one TE type. Our results show that TEs are causative agents of genetic change that result in differentiation between island and mainland populations. This substrate of genetic novelty appears to be a key source of variation as populations adapt to new environments, especially on short

timescales.

Local Adaptation with Standing Variation or New Mutations

Adaptation during shifts in selective pressures can come from standing variation or from new mutations [10, 20, 68]. Standing variation in populations is immediately available for adaptation, and may proceed to fixation so long as allele frequencies are high enough to establish deterministic selective sweeps [11]. New mutations are expected to appear more slowly, as mutations accumulate in clock-like fashion as generations progress. The relative contribution of new mutation and standing variation can tell us how quickly populations are able to evolve genetic solutions in populations as they adapt to new habitats. The spectrum of neutral diversity segregating in natural populations depends on the effective population size, and the mutation rate, where $\pi = \theta = 4N_e * \mu$. Larger populations will weed out mutations with large detrimental impacts where $4N_e * s > 1$, limiting the span of variation.

In our analysis of chromosomal rearrangements, we observe differentiation with large Δp and F_{ST} within a time-span of 500,000 years [28]. Here, we observe the majority of rearrangements (76.2%) are derived from new mutations not present on the mainland. However, standing variation is associated with more dynamic differentiation, with larger values of Δp than new mutations. Our results imply that the tempo of local adaptation is then expected to proceed in two waves. First, an initial spread of standing variation after habitat invasion leads to adaptation from the limited span of mutations imported from the founder population. In such a case, we expect genetic differentiation at multiple loci shortly after invasion. Still, the substrate available among standing variation is insufficient to facilitate adaptation to the optimum. Afterwards, new mutations appear stochastic ally in the population, and spread if selectively favored.

At SNPs, long wait times would affect the span of adaptation, as multiple generations are expected to be required before establishment of deterministic sweeps [4, 11, 69, 70]. However, TE-induced mutations can be generated in “bursts” that remodel genomes with many mutations at once [71]. Our results suggest that new mutations from transposable have rapidly changed genome content and structure, as they move pieces of DNA around the genome [72]. These genetic responders serve as a source of increased variation that fortuitously creates novel substrates, including genetic changes at UV tolerance loci. The subset of selectively favored mutations is a minority of the genetic diversity identified (244/16480 rearrangements 1.480%). The large number of mutations that must be sifted through suggests that adaptation is a game of genetic chance, where the dice must be rolled multiple times for organisms to achieve selective advantages.

Methods

Whole genome sequencing and SNP calling

We generated whole genome sequencing for single *Drosophila* from 42 strains of *D. santomea* from São Tomè, 35 strains of *D. yakuba* from the island of São Tomè, and 19 strains of *D. yakuba* from the central African mainland (Cameroon and Kenya). DNA was extracted from flies flash frozen in liquid nitrogen following QIAamp Mini Kit (Qiagen) protocol without

using RNase A. The resulting DNA samples were quantified (Qubit dsDNA HS assay kit, ThermoFisher Scientific), assessed for quality (Nanodrop ND-2000; A260/A280>1.8), and stored at -20°C.

Illumina TruSeq Nano DNA libraries were prepared manually following the manufacturer’s protocol (TruSeq Nano DNA, RevD; Illumina). Briefly, samples were normalized to 100ng DNA and sheared by sonication with Covaris M220 (microTUBE 50; Sage Science). The samples were end repaired, purified with Ampure XP beads (Agencourt; Beckman Coulter), adaptors adenylated, and Unique Dual Indices (Table) ligated. Adaptor enrichment was performed using eight cycles of PCR. Following Ampure XP bead cleanup, fragment sizes for all libraries were measured using Agilent Bioanalyzer 2100 (HS DNA Assay; Applied Biosystems). The libraries were diluted 1:10 000 and 1:20 000 and quantified in triplicate using the KAPA Library Quantification Kit (Kapa Biosystems). Equimolar samples were pooled and the libraries were size selected targeting 400-700bp range to remove adaptor monomers and dimers using Pippin Prep DNA Size Selection system (1.5% Agarose Gel Cassette #CDF1510; Sage Sciences). Library pools (24 samples per lane) were run on an Illumina HiSeq 4000 platform using the 150bp paired end (PE) Cluster Kit.

We aligned short read sequences to the *D. yakuba* reference genome r1.0.5 and *Wolbachia* endoparasite sequence NC_002978.6 using bwa aln, and resolved paired end mappings using bwa sampe. We sorted alignments by position using samtools sort. Sequence depth on sorted bam files was calculated using samtools depth -aa.

Using GATK [18] we called the SNPs for each strain. To calculate the frequency we need to determine the haplotype, which we do using an HMM. After initially running the HMM with incorrect parameters we observe no changes of state, so we used the Baum-Welsh algorithm to estimate the parameters of the HMM. With the correct parameters we can rerun the HMM and determine haplotypes for SNPs and calculate their frequencies.

HiFi PacBio sequences were used to confirm the Illumina structural variant calls. We call structural variants using minimap2 [36], Sniffles [37], and PacBip’s pbsv [38]. All structural variant calls were done with alignments created by minimap2, except in the case of pbsv which requires alignments from pbmm2 [38], a Minimap2 frontend for PacBio native data formats.

Identification of chromosomal rearrangements

We identified abnormally mapping read pairs on different chromosomes and long-spanning read pairs greater than 100kb apart as signals of putative chromosomal rearrangements. Mutations with greater than 3 read pairs supporting were included among the chromosomal rearrangements. The mutation data were then clustered across strains assuming that variants were within 325 base pairs of each other on from either rearrangement breakpoint. Taking the min and max for each of the rearrangement’s breakpoints in a cluster, we associate all strains in said cluster with these bounds.

D. yakuba is resistant to inbreeding due to segregating inversions [26, 73, 74]. To identify inbred and heterozygous regions and correct allele frequencies, we used a Hidden Markov Model (HMM) to parse SNP heterozygosity for each strain. In *D. yakuba*, some strains had reference strain contamination, resulting in no heterozygous or homozygous non-reference SNPs. In *D. santomea* no indication of reference contamination was observed. We used a

three state HMM for *D. yakuba* and an two-state HMM for *D. santomea* to identify reference contamination, inbred haplotypes, and non-inbred haplotypes. Transitions probabilities were set to 10^{-10} . Emission probabilities were set as heterozygosity for inbred regions would be 0, and heterozygosity in non-inbred regions was $\theta = 0.01$, with a lower threshold for probabilities on off-diagonals of $\epsilon = 0.00005$ to prevent chilling effects of zero probability.

Haplotype calls from the HMM were used to generate correct site frequency spectra for SNPs and structural variants given the variable number of chromosomes sampled across different parts of the genome.

Within inbred regions, we assume mutations are homozygous, and assign a genotype of 1 structural variant on 1 sampled chromosome. Within heterozygous haplotypes, read pair information alone cannot detect ploidy. For outbred regions with two chromosomes with different ancestry, we used coverage changes to distinguish hemizygous and homozygous mutations. We compared the average coverage of observed mutations to the average coverage across the entire chromosome in a strain looking for an observed coverage between $1.45 < x < 1.55$ or $1.95 < x < 2.05$. Regions whose haplotypes were around 1.5x the average coverage of the chromosome are expected to be heterozygous, and regions who have around 2x the average are expected to be homozygous. False negative genotypes are possible when read pair support is insufficient to identify rearrangements de novo. For each mutation, if another strain showed 1.5x or 2x coverage changes and lesser support of 1 or 2 read pairs, allele frequencies were adjusted to avoid low frequency reads, similarly to prior work on gene duplications and rearrangements [20, 26].

Polarize ancestral state

Genotyping identifies mutations in populations that differ from the reference sequence, but on its own cannot identify which is ancestral and which is novel. To determine the ancestral state for rearrangements, we compared each variant to *D. teissieri*, we determine whether mutations are novel or if the ancestral state has been rearranged in the reference strain. To polarize the mutations we use BLASTn at an E-value of 10^{-20} to compare the *D. yakuba* reference sequence for +/- 1kb of each rearrangement breakpoint to *D. teissieri*. We consider a mutation the ancestral state if both sequences map to the same location in *D. teissieri*, they have an alignment length greater than 150, share greater than 95 percent identity, and the two sequences overlap less than 10 percent in *D. teissieri*. Mutations where samples were identified as containing the ancestral state found in *D. teissieri*, allele frequencies from genotyping, p , were reversed to $(1 - p)$ to reflect the reference as the new mutation.

By using the haplotype data we determine the number of sampled strains and compare them to the number of observed strains in the clustered rearrangements .

Association with transposable elements

To match variants with transposable elements (TEs) we used BLAST to compare the variants to Repbase. Variants that mapped to TEs at an e-value of 10^{-20} were marked as TEs in our analysis. By using BLAST to compare both the origin and destination loci of the variant, we were able to see which variants mapped on either one or both sides of the rearrangement.

(This was verified by checking the regions to make sure that they had unusual coverage compared to the average for that chromosome and strain.)

Resolving complex variation

Previous work has shown that Pacbio can confirm 100% of Illumina paired-end reads when using alignment methods in tandem, as the rate varies on the confirmation method (BLAST, MM2, PBSV, etc). (Figure S20). The majority of unconfirmed regions have erratic coverage, implying complex variation that the aligners and assemblers cannot solve. To investigate further, we conducted targeted *de novo* assembly of these regions and plotted them with Mummer.

Structural variant allele frequencies

We used polarized allele frequencies adjusted for inbreeding to calculate the allele frequency for each of the variants that we observed. We calculated the allele frequency within sub-populations for *D. santomea*, island *D. yakuba* and mainland *D. yakuba*. With the allele frequency data for each variant and the separation by sub-population. To generate an SFS while accounting for uneven sample sizes across the genome, we projected allele frequencies in each subpopulation to a sample size of $n=19$ using a hypergeometric model [26, 75].

Differentiation between populations is a signature of local adaptation to changing environments. This differentiation can be measured through different means. This study benefits from a known ancestral mainland population that invaded new island environments that can be used as a population genetic ‘control’ to identify allele frequency changes. Simulations from other groups have shown that the difference in allele frequencies, Δp

$$p_1 - p_2 \tag{1}$$

and F_{ST}

$$\frac{\bar{p}(1 - \bar{p}) - \sum c_i p_i (1 - p_i)}{\bar{p}(1 - \bar{p})} \tag{2}$$

can identify population differentiation during local adaptation. Δp , and F_{ST} contain overlapping information. Δp contains directionality that F_{ST} lacks, and may be more useful on moderate timescales when populations have had sufficient time for variants to spread in populations. It may identify population differentiation better than F_{ST} while F_{ST} may be more sensitive to changes while allele frequencies are low. We calculate Δp and F_{ST} identify structural variants that have spread in island environments.

To determine whether mutations showed unusually high population differentiation we calculated a Bonferroni corrected 95% confidence interval, calculated by chromosome due to the distribution of Δp varying by chromosome. Mutations that were greater than the upper bound of the C.I were considered significantly differentiated.

SNP Population diversity

To measure the selective pressure and genomic structural differences caused by the rearrangements we calculate Θ_π , Θ_w , and Tajima’s D . These statistics are calculated for a 10kb

sliding window with a 1kb slide. Using these estimates we matched our variants into these windows and associated the rearrangement with the window whose midpoint was closest to the origin locus.

Gene ontology

Using the location of the rearrangements we looked 5kb upstream and downstream of the mutations to see if there were genes that could be affected. Variants that matched *D. yakuba* gene coordinates were mapped to their orthologs in *D. melanogaster* using Flybase [76]. Genes that had no orthologs were excluded. Using these orthologs we analyzed the functional gene annotations using DAVID [77] using low stringency.

Tissue dissection and RNA sequencing

To determine how rearrangements might change gene expression profiles or create new genes, we collected RNAseq data for a subset of 14 strains. Because new gene formation commonly occurs at genes with testes-specific expression [78–81] we collected gene expression data for gonads and soma of adult male and female flies. For each strain, we collected virgin males and females within 2 hours of eclosion and placed into separate vials to age for 5-7 days. Once adults, we placed individual males and females on a glass slide with Ringer’s solution for gonad dissection. We removed testes and the accessory gland from males and the ovaries from females. Gonads and the carcass (rest of the body minus the gonads) were placed into separate Eppendorf tubes and flash frozen immediately in liquid nitrogen. Five biological replicates were used for each tissue.

RNA was extracted from fly tissue frozen in liquid nitrogen following Zymo DirectZol RNA Microprep (Zymo Research) without DNAase treatment. The resulting RNA samples were quantified (Qubit RNA HS assay kit, ThermoFisher Scientific), assessed for quality (Nanodrop ND-2000; A260/A280>2.0), and stored at -80°C.

Poly (A) enriched strand-specific Illumina TruSeq libraries were manually prepared following the manufacturer’s protocol (TruSeq Stranded mRNA LS, RevD; Illumina). Briefly, samples were normalized to 100ng RNA and poly (A) containing mRNA molecules purified using poly (T) oligo attached magnetic beads. The poly (A) molecules were chemically fragmented for 8 minutes and primed for cDNA synthesis. Reverse transcription was performed using SuperScript IV enzyme (Invitrogen), samples purified with Ampure XP beads (Agencourt; Beckman Coulter), adaptors adenylated, and Unique Dual Indices (Table) ligated. Adaptor enrichment was performed using 15 cycles of PCR. Following Ampure XP bead cleanup, fragment sizes for all libraries were measured using Agilent Bioanalyzer 2100 (HS DNA Assay; Applied Biosystems). The libraries were diluted 1:10 000 and 1:20 000 and quantified in triplicate using the KAPA Library Quantification Kit (Kapa Biosystems). Equimolar samples were pooled (20 samples per lane) and run on an Illumina HiSeq 4000 platform using the 150bp paired end (PE) Cluster Kit.

Identifying chromosomal rearrangements and differential expression analysis

To determine if strains contain structural rearrangements, we performed a Tophat fusion search version 2.1.0 to find split reads on paired-end RNA sequencing data [50]. This program has previously been validated to identify chimeric constructs using split-read mapping and abnormal read pairs in RNASeq data at loci with genomic DNA signals indicating rearrangements [4, 21, 26]. We identified genes within 5kb of rearrangement breakpoints to identify genes most likely to experience changes in gene expression. We then identified structural variants that were differentially expressed using the program CuffDiff [82]. To determine whether gene expression changes and fusion transcripts are associated with local adaptation, these were also examined for signatures of selection.

We separated structural variant data into male carcass, female carcass, male gonads, and female gonads to determine if these differed across the tissue sample. To identify statistically significant expression changes across the structural variants, we calculated Fisher's Adjusted P-values [83] using the p-values for expression in each strain that contained that structural variant. To determine whether structural variants as a class are more likely to induce changes in gene expression than we would expect for the genome at large, we performed 10,000 bootstrap replicates with random sampling of 9549 to 10632 genes depending on the tissue.

Acknowledgements

This work was funded by NIH NIGMS MIRA R35-GM133376 to Rebekah L. Rogers and by startup funding from the University of North Carolina, Charlotte. TM is funded by UGA Training Grant T32GM007103 from NIH NIGMS and NSF DEB-1737824 to Kelly Dyer.

Data Availability

All sequence data are available under SRA PRJNA764098, PRJNA764689, PRJNA764691, PRJNA764693, PRJNA764695, PRJNA764098, PRJNA269314. Supplementary Data are available at <https://www.dropbox.com/sh/4fkf4fojcbbnzil/AABpp5TGefHjaQk1YqI9bPKa?dl=0>.

References

- [1] Schoville SD, et al. (2012) Adaptive genetic variation on the landscape: methods and cases. *Annual Review of Ecology, Evolution, and Systematics* 43:23–43.
- [2] Ohno S (2013) *Evolution by gene duplication*. (Springer Science & Business Media).
- [3] Conant GC, Wolfe KH (2008) Turning a hobby into a job: how duplicated genes find new functions. *Nature Reviews Genetics* 9(12):938–950.
- [4] Rogers RL, Shao L, Thornton KR (2017) Tandem duplications lead to novel expression patterns through exon shuffling in *Drosophila yakuba*. *PLoS Genetics* 13(5):e1006795.
- [5] Rogers RL, Hartl DL (2012) Chimeric genes as a source of rapid evolution in *Drosophila melanogaster*. *Molecular biology and evolution* 29(2):517–529.
- [6] Kondrashov FA, Kondrashov AS (2006) Role of selection in fixation of gene duplications. *Journal of Theoretical Biology* 239(2):141–151.
- [7] Huminiecki L, Wolfe KH (2004) Divergence of spatial gene expression profiles following species-specific gene duplications in human and mouse. *Genome Research* 14(10a):1870–1879.
- [8] Harewood L, Fraser P (2014) The impact of chromosomal rearrangements on regulation of gene expression. *Human Molecular Genetics* 23(R1):R76–R82.
- [9] De S, Teichmann SA, Babu MM (2009) The impact of genomic neighborhood on the evolution of human and chimpanzee transcriptome. *Genome Research* 19(5):785–794.
- [10] Barrett RD, Schluter D (2008) Adaptation from standing genetic variation. *Trends in Ecology & Evolution* 23(1):38–44.
- [11] Hermisson J, Pennings PS (2005) Soft sweeps: molecular population genetics of adaptation from standing genetic variation. *Genetics* 169(4):2335–2352.
- [12] Orr HA (2005) The genetic theory of adaptation: a brief history. *Nature Reviews Genetics* 6(2):119–127.
- [13] Coyne JA, Orr HA (1989) Patterns of speciation in *Drosophila*. *Evolution* 43(2):362–381.
- [14] Ohta T (1992) The nearly neutral theory of molecular evolution. *Annual Review of Ecology and Systematics* 23(1):263–286.
- [15] Lynch M, et al. (1999) Perspective: spontaneous deleterious mutation. *Evolution* 53(3):645–663.
- [16] Kimura M, , et al. (1968) Evolutionary rate at the molecular level. *Nature* 217(5129):624–626.

- [17] Smith JM, Haigh J (1974) The hitch-hiking effect of a favourable gene. *Genetics Research* 23(1):23–35.
- [18] McKenna A, et al. (2010) The genome analysis toolkit: a mapreduce framework for analyzing next-generation DNA sequencing data. *Genome Research* 20(9):1297–1303.
- [19] Li H (2011) A statistical framework for SNP calling, mutation discovery, association mapping and population genetical parameter estimation from sequencing data. *Bioinformatics* 27(21):2987–2993.
- [20] Rogers RL, et al. (2014) Landscape of standing variation for tandem duplications in *Drosophila yakuba* and *Drosophila simulans*. *Molecular Biology and Evolution* 31(7):1750–1766.
- [21] Rogers RL (2015) Chromosomal rearrangements as barriers to genetic homogenization between archaic and modern humans. *Molecular Biology and Evolution* 32(12):3064–3078.
- [22] Ellegren H (2014) Genome sequencing and population genomics in non-model organisms. *Trends in Ecology & Evolution* 29(1):51–63.
- [23] Clark AG, et al. (2007) Evolution of genes and genomes on the drosophila phylogeny. *Nature* 450(7167):203–218.
- [24] Bhutkar A, et al. (2008) Chromosomal rearrangement inferred from comparisons of 12 drosophila genomes. *Genetics* 179(3):1657–1680.
- [25] Ranz JM, Castillo-Davis CI, Meiklejohn CD, Hartl DL (2003) Sex-dependent gene expression and evolution of the *Drosophila* transcriptome. *Science* 300(5626):1742–1745.
- [26] Stewart NB, Rogers RL (2019) Chromosomal rearrangements as a source of new gene formation in *Drosophila yakuba*. *PLoS Genetics* 15(9):e1008314.
- [27] Lachaise D, et al. (2000) Evolutionary novelties in islands: *Drosophila santomea*, a new melanogaster sister species from sao tome. *Proceedings of the Royal Society of London. Series B: Biological Sciences* 267(1452):1487–1495.
- [28] Coyne JA, Kim SY, Chang AS, Lachaise D, Elwyn S (2002) Sexual isolation between two sibling species with overlapping ranges: *Drosophila santomea* and *Drosophila yakuba*. *Evolution* 56(12):2424–2434.
- [29] Llopart A, Lachaise D, Coyne JA (2005) An anomalous hybrid zone in *Drosophila*. *Evolution* 59(12):2602–2607.
- [30] Obbard DJ, et al. (2012) Estimating divergence dates and substitution rates in the *Drosophila* phylogeny. *Molecular Biology and Evolution* 29(11):3459–3473.

- [31] Cariou ML, Silvain JF, Daubin V, Da Lage JL, Lachaise D (2001) Divergence between *Drosophila santomea* and allopatric or sympatric populations of *D. yakuba* using paralogous amylase genes and migration scenarios along the cameroon volcanic line. *Molecular Ecology* 10(3):649–660.
- [32] Comeault AA, Venkat A, Matute DR (2016) Correlated evolution of male and female reproductive traits drive a cascading effect of reinforcement in *drosophila yakuba*. *Proceedings of the Royal Society B: Biological Sciences* 283(1835):20160730.
- [33] Bachtrog D, Thornton K, Clark A, Andolfatto P (2006) Extensive introgression of mitochondrial DNA relative to nuclear genes in the *Drosophila yakuba* species group. *Evolution* 60(2):292–302.
- [34] Andolfatto P, Wong KM, Bachtrog D (2011) Effective population size and the efficacy of selection on the x chromosomes of two closely related *drosophila* species. *Genome Biology and Evolution* 3:114–128.
- [35] Llopart A, Elwyn S, Lachaise D, Coyne JA (2002) Genetics of a difference in pigmentation between *drosophila yakuba* and *drosophila santomea*. *Evolution* 56(11):2262–2277.
- [36] Li H (2018) Minimap2: pairwise alignment for nucleotide sequences. *Bioinformatics* 34(18):3094–3100.
- [37] Sedlazeck FJ, et al. (2018) Accurate detection of complex structural variations using single-molecule sequencing. *Nature Methods* 15(6):461–468.
- [38] Wenger AM (year?) Comprehensive structural and copy-number variant detection with long reads.
- [39] Rogers RL, et al. (2015) Tandem duplications and the limits of natural selection in *drosophila yakuba* and *drosophila simulans*. *PLoS One* 10(7):e0132184.
- [40] Montgomery E, Huang S, Langley C, Judd B (1991) Chromosome rearrangement by ectopic recombination in *Drosophila melanogaster*: genome structure and evolution. *Genetics* 129(4):1085–1098.
- [41] Jurka J, et al. (2005) Repbase update, a database of eukaryotic repetitive elements. *Cytogenetic and Genome Research* 110(1-4):462–467.
- [42] Mérel V, Boulesteix M, Fablet M, Vieira C (2020) Transposable elements in *Drosophila*. *Mobile DNA* 11(1):1–20.
- [43] Villanueva-Cañas JL, Horvath V, Aguilera L, González J (2019) Diverse families of transposable elements affect the transcriptional regulation of stress-response genes in *Drosophila melanogaster*. *Nucleic Acids Research* 47(13):6842–6857.
- [44] Fawcett JA, Innan H (2019) The role of gene conversion between transposable elements in rewiring regulatory networks. *Genome Biology and Evolution* 11(7):1723–1729.

- [45] Innan H, Kim Y (2008) Detecting local adaptation using the joint sampling of polymorphism data in the parental and derived populations. *Genetics* 179(3):1713–1720.
- [46] Halligan DL, Keightley PD (2006) Ubiquitous selective constraints in the drosophila genome revealed by a genome-wide interspecies comparison. *Genome Research* 16(7):875–884.
- [47] Llopart A (2012) The rapid evolution of X-linked male-biased gene expression and the large-x effect in *Drosophila yakuba*, *D. santomea*, and their hybrids. *Molecular Biology and Evolution* 29(12):3873–3886.
- [48] Matute DR, Gavin-Smyth J (2014) Fine mapping of dominant X-linked incompatibility alleles in *Drosophila* hybrids. *PLoS Genetics* 10(4):e1004270.
- [49] Trapnell C, et al. (2010) Transcript assembly and quantification by RNA-Seq reveals unannotated transcripts and isoform switching during cell differentiation. *Nature Biotechnology* 28(5):511–515.
- [50] Kim D, Salzberg SL (2011) Tophat-fusion: an algorithm for discovery of novel fusion transcripts. *Genome Biology* 12(8):1–15.
- [51] Carvunis AR, et al. (2012) Proto-genes and *de novo* gene birth. *Nature* 487(7407):370–374.
- [52] Matute DR, Butler IA, Coyne JA (2009) Little effect of the *tan* locus on pigmentation in female hybrids between *Drosophila santomea* and *D melanogaster*. *Cell* 139(6):1180–1188.
- [53] Rebeiz M, et al. (2009) Evolution of the *tan* locus contributed to pigment loss in *Drosophila santomea*: a response to Matute et al. *Cell* 139(6):1189–1196.
- [54] Pennings PS, Hermisson J (2006) Soft sweeps iii: the signature of positive selection from recurrent mutation. *PLoS Genetics* 2(12):e186.
- [55] Harr B, Todorova J, Schlötterer C (2002) Mismatch repair-driven mutational bias in *d. melanogaster*. *Molecular Cell* 10(1):199–205.
- [56] Broderick S, Wang X, Simms N, Page-McCaw A (2012) *Drosophila Ninjurin A* induces nonapoptotic cell death. *PLoS One*.
- [57] Neufeld TP, Rubin GM (1994) The *Drosophila peanut* gene is required for cytokinesis and encodes a protein similar to yeast putative bud neck filament proteins. *Cell* 77(3):371–379.
- [58] Rech GE, et al. (2019) Stress response, behavior, and development are shaped by transposable element-induced mutations in drosophila. *PLoS Genetics* 15(2):e1007900.
- [59] Heck BW, et al. (2011) The transcriptional corepressor smrter influences both notch and ecdysone signaling during drosophila development. *Biology Open* 1(3):182–196.

- [60] Bastide H, Yassin A, Johanning EJ, Pool JE (2014) Pigmentation in *Drosophila melanogaster* reaches its maximum in Ethiopia and correlates most strongly with ultraviolet radiation in sub-Saharan Africa. *BMC Evolutionary Biology* 14(1):1–14.
- [61] Brodsky MH, et al. (2000) *Drosophila* p53 binds a damage response element at the reaper locus. *Cell* 101(1):103–113.
- [62] Vaisnav M, et al. (2014) Genome-wide association analysis of radiation resistance in *Drosophila melanogaster*. *PLoS One* 9(8):e104858.
- [63] Flores C, Engels W (1999) Microsatellite instability in *Drosophila spellchecker1* (MutS homolog) mutants. *Proceedings of the National Academy of Sciences* 96(6):2964–2969.
- [64] Carbone MA, Llopart A, DeAngelis M, Coyne JA, Mackay TF (2005) Quantitative trait loci affecting the difference in pigmentation between *Drosophila yakuba* and *D. santomea*. *Genetics* 171(1):211–225.
- [65] Laudencia-Chingcuanco D, Fowler DB (2012) Genotype-dependent burst of transposable element expression in crowns of hexaploid wheat (*Triticum aestivum* L.) during cold acclimation. *Comparative and Functional Genomics* 2012.
- [66] Lynch VJ, Leclerc RD, May G, Wagner GP (2011) Transposon-mediated rewiring of gene regulatory networks contributed to the evolution of pregnancy in mammals. *Nature Genetics* 43(11):1154–1159.
- [67] Feschotte C (2008) Transposable elements and the evolution of regulatory networks. *Nature Reviews Genetics* 9(5):397–405.
- [68] Assis R, Bachtrog D (2013) Neofunctionalization of young duplicate genes in *Drosophila*. *Proceedings of the National Academy of Sciences* 110(43):17409–17414.
- [69] Smith JM (1971) What use is sex? *Journal of Theoretical Biology* 30(2):319–335.
- [70] Gillespie JH (1994) *The causes of molecular evolution*. (Oxford University Press On Demand) Vol. 2.
- [71] Cridland JM, Macdonald SJ, Long AD, Thornton KR (2013) Abundance and distribution of transposable elements in two *Drosophila* QTL mapping resources. *Molecular Biology and Evolution* 30(10):2311–2327.
- [72] Guerreiro MPG (2014) Interspecific hybridization as a genomic stressor inducing mobilization of transposable elements in *Drosophila*. *Mobile Genetic Elements* 4(4):e88992.
- [73] Guillén Y, Ruiz A (2012) Gene alterations at *Drosophila* inversion breakpoints provide prima facie evidence for natural selection as an explanation for rapid chromosomal evolution. *BMC Genomics* 13(1):1–18.
- [74] Andolfatto P (2001) Contrasting patterns of X-linked and autosomal nucleotide variation in *Drosophila melanogaster* and *Drosophila simulans*. *Molecular Biology and Evolution* 18(3):279–290.

- [75] Nielsen R (2005) Molecular signatures of natural selection. *Annu. Rev. Genet.* 39:197–218.
- [76] Drysdale R, Consortium F, , et al. (2008) Flybase. *Drosophila* pp. 45–59.
- [77] Sherman BT, Lempicki RA, , et al. (2009) Systematic and integrative analysis of large gene lists using DAVID bioinformatics resources. *Nature Protocols* 4(1):44–57.
- [78] Zhou Q, et al. (2008) On the origin of new genes in *Drosophila*. *Genome Research* 18(9):1446–1455.
- [79] Rogers RL, Shao L, Sanjak JS, Andolfatto P, Thornton KR (2014) Revised annotations, sex-biased expression, and lineage-specific genes in the *Drosophila melanogaster* group. *G3: Genes, Genomes, Genetics* 4(12):2345–2351.
- [80] Betrán E, Thornton K, Long M (2002) Retroposed new genes out of the X in *Drosophila*. *Genome Research* 12(12):1854–1859.
- [81] Bachtrog D, Toda NR, Lockton S (2010) Dosage compensation and demasculinization of X chromosomes in *Drosophila*. *Current Biology* 20(16):1476–1481.
- [82] Trapnell C, et al. (2012) Differential gene and transcript expression analysis of RNA-seq experiments with tophat and cufflinks. *Nature Protocols* 7(3):562–578.
- [83] Tsuyuzaki K, Nikaido I (2013) metaseq: Meta-analysis of RNA-seq count data. *Tokyo University of Science, Tokyo*.

Table 1: Number of rearrangements by breakpoint chromosomes.

Population	2L	2R	3L	3R	X
Meta-population	6,338	5,597	5,279	6,633	4,818
<i>D. santomea</i>	3,301	2,792	2,475	3,037	2,152
Island <i>D. yakuba</i>	2,600	2,340	2,155	3,017	2,020
Mainland <i>D. yakuba</i>	1,176	1,047	1,105	1,225	1,186

Table 2: Number of genes withing 5kb of a rearrangement breakpoint

Population	2L	2R	3L	3R	X
Meta-population	742	641	674	844	552
<i>D. santomea</i>	557	279	441	509	324
Island <i>D. yakuba</i>	505	322	456	642	328
Mainland <i>D. yakuba</i>	343	298	273	337	261

Table 3: Number of rearrangement by breakpoint chromosomes associated with TEs

Population	2L	2R	3L	3R	X
Meta-population	5,510	4,841	4,426	5,710	3,667
<i>D. santomea</i>	2,944	2,540	2,227	2,707	1,721
Island <i>D. yakuba</i>	2,280	2,019	1,787	2,600	1,534
Mainland <i>D. yakuba</i>	959	805	817	995	757

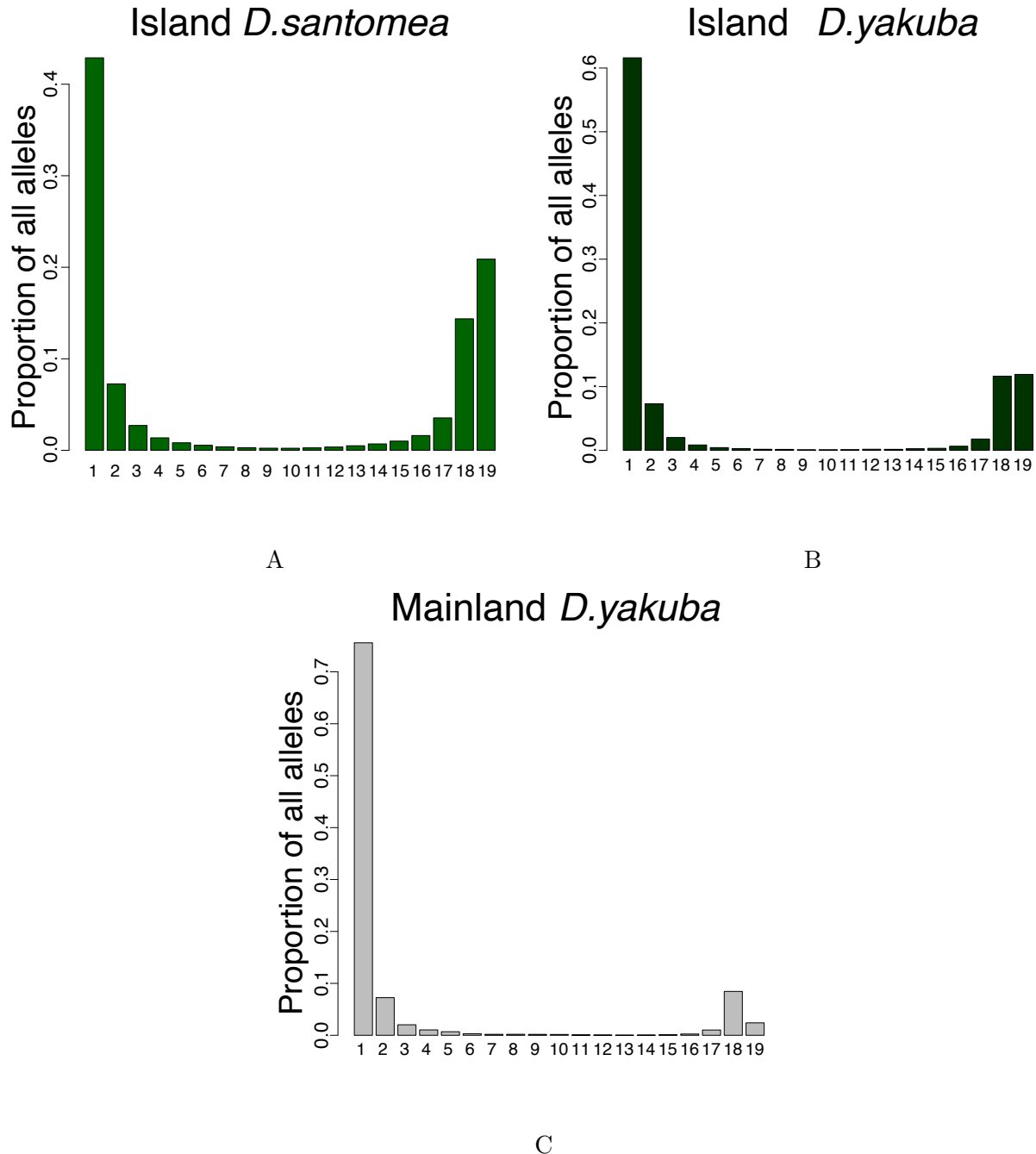


Figure 1: A) Site frequency spectrum of *D. santomea*. Polarized ancestral state with *D. teissieri* and projected down to $n=19$ using the geometric distribution. The increase in high frequency variants is much greater than that of the mainland *D. yakuba* B) Site frequency spectrum of the island *D. yakuba*. Polarized ancestral state with *D. teissieri* and projected down to $n=19$ using the geometric distribution. The increase in high frequency variants is slightly greater than that of the mainland *D. yakuba*, but not as much as *D. santomea*, likely related to divergence time C) Site frequency spectrum of mainland *D. yakuba*. Polarized ancestral state with *D. teissieri* and projected down to $n=19$ using the hypergeometric distribution. Lacks the increase in high frequency variants that is present in both of the other sub-populations.

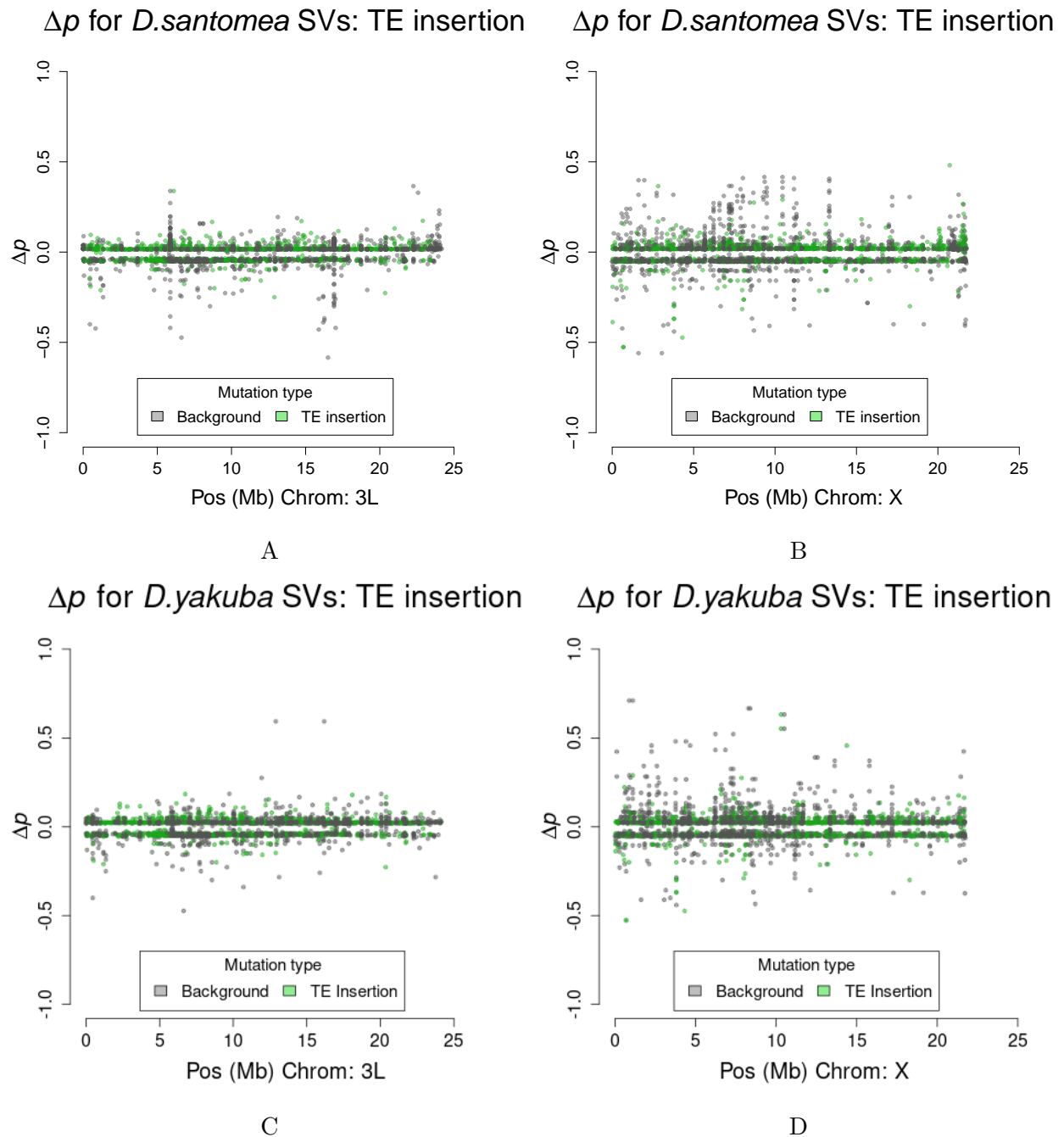


Figure 2: Population differentiation as shown via Δp A) Between *D. santomea* and mainland ancestral *D. yakuba* on autosome 3L. B) Between *D. santomea* and mainland ancestral *D. yakuba* on the X chromosome C) Between Island *D. yakuba* and ancestral mainland *D. yakuba* on the autosome 3L. D) Between Island *D. yakuba* and ancestral mainland *D. yakuba* on the X chromosome. The x-axis shows genomic position on the chromosome in megabases, and the y-axis is difference in allele frequencies between the test population and the mainland. Points in light green highlight the rearrangements associated with new TE insertions. We observe greater levels of differentiation on the X compared to the autosomes in both populations.

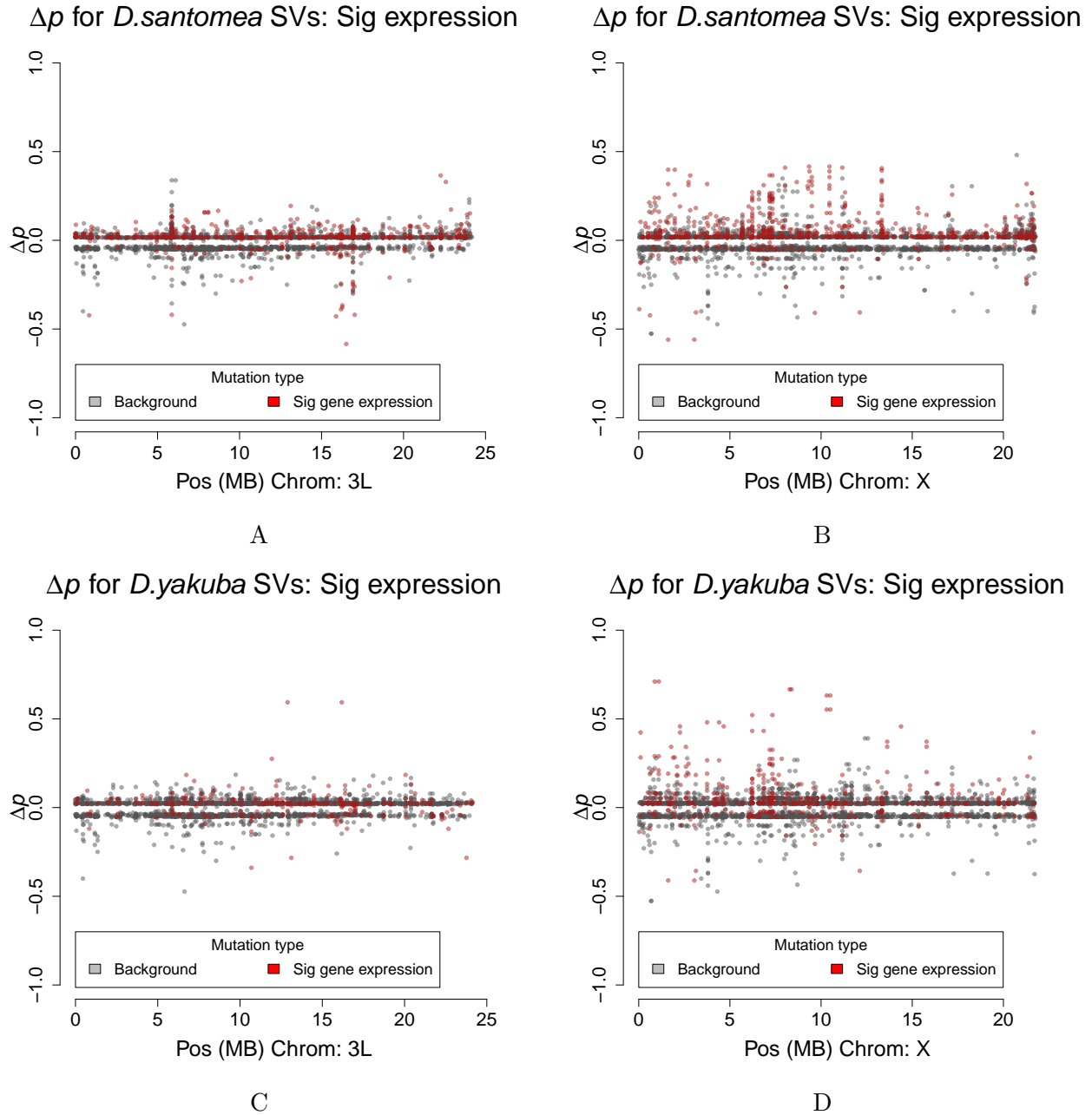


Figure 3: Population differentiation as shown via Δp A) Between *D. santomea* and mainland ancestral *D. yakuba* on autosome 3L. B) Between *D. santomea* and mainland ancestral *D. yakuba* on the X chromosome C) Between Island *D. yakuba* and ancestral mainland *D. yakuba* on the autosome 3L. D) Between Island *D. yakuba* and ancestral mainland *D. yakuba* on the X chromosome. The x-axis shows genomic position on the chromosome in megabases, and the y-axis is difference in allele frequencies between the test population and the mainland. Points in red highlight the rearrangements associated with significant gene expression. We observe greater levels of differentiation on the X compared to the autosomes in both populations and rearrangements associated with significant expression changes on the X show strong differentiation. These results suggest that gene expression changes induced by rearrangements are important for local adaptation.

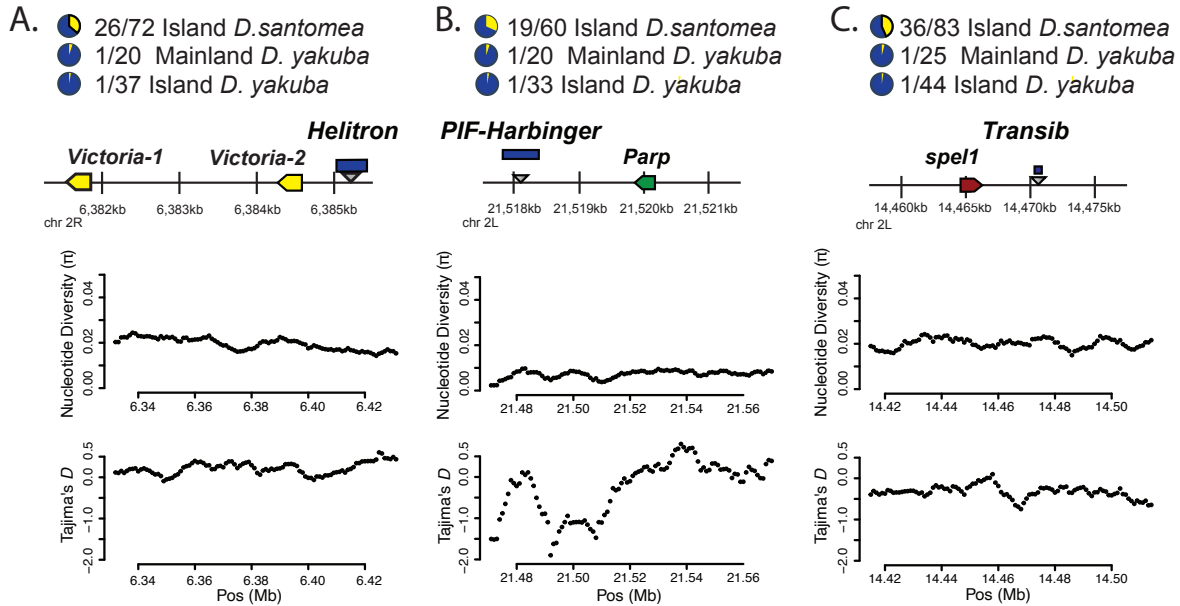


Figure 4: High altitude *D. santomea* experience greater UV exposure. Three genes show rearrangements associated with UV tolerance genes in high altitude *D. santomea* as shown via A) Multiple rearrangements associated with *Victoria*, which are mediated by a *Helitron* element, and drops in π and Tajima's (D) (local minima $\pi=0.0160$ and $D=-0.0917$) B) Multiple rearrangements associated with *Parp*, which are mediated by a *Harbinger* element, and drops in π and Tajima's (D) (local minima $\pi=0.00134$ and $D=-1.89$). C) Multiple rearrangements associated with *spel1*, which are mediated by a *Transib* element, and drops in π and Tajima's (D) (local minima $\pi=0.0135$ and $D=-0.748$). For each of the three genes at least one rearrangement show a large shift in allele frequency and have statistically significant Δp . *Parp* and *spel1* also show significant differential gene expression via Fisher's combined p-values. Genomic averages for π and Tajima's D are $\pi=0.0159$ and $D=-0.0445$

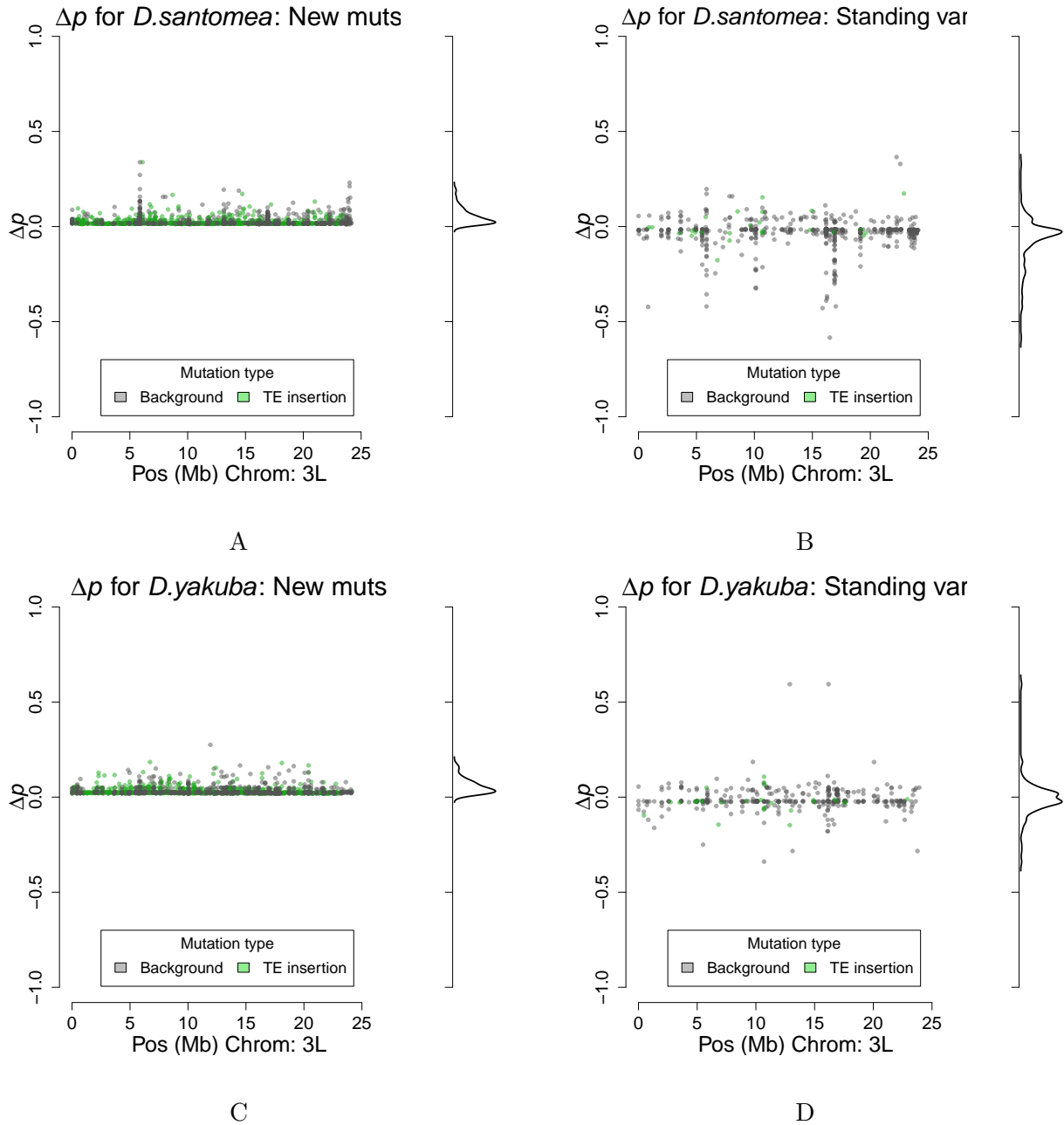


Figure 5: Population differentiation as shown via Δp A) Between *D. santomea* and mainland ancestral *D. yakuba* for new mutations identified on autosome 3L. B) Between *D. santomea* and mainland ancestral *D. yakuba* for standing variation identified on autosome 3L. C) Between Island *D. yakuba* and ancestral mainland *D. yakuba* for new mutations on the autosome 3L. D) Between Island *D. yakuba* and ancestral mainland *D. yakuba* for standing variation on the 3L. The x-axis shows genomic position on the chromosome in megabases, and the y-axis is difference in allele frequencies between the test population and the mainland. Points in light green highlight the rearrangements associated with new TE insertions. Standing variation shows greater differentiation, consistent with longer timescales for fixation. However, many variants that appeared as new mutation TE lead to population differentiation. These results suggest that new mutations, especially TE induced mutations, can contribute to genetic changes during habitat invasion.

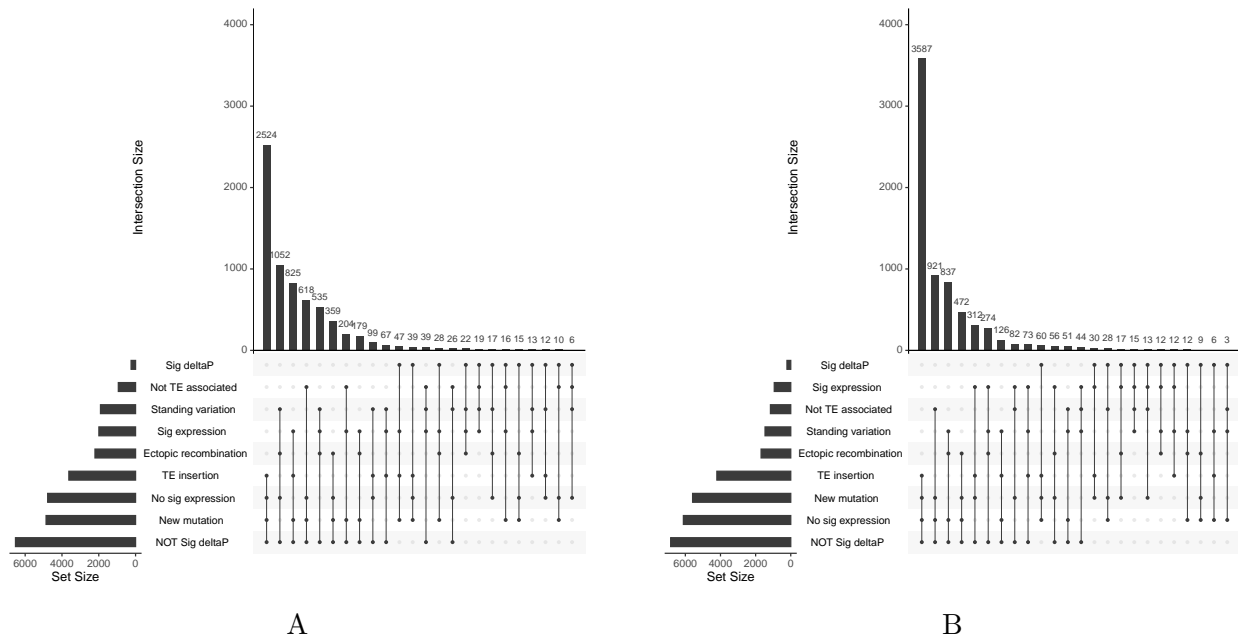


Figure 6: Upset plot showing factors associated with rearrangements. Novel TE insertions without population differentiation and without changes in gene expression are the most common type of mutation in (A) *D. santomea* and (B) *D. yakuba*. New mutations induced by TE insertion with significant changes in gene expression are the most common type of variation that contributes to population differentiation.

Supplementary Information

Complex variation causes genotyping challenges

Long read sequencing is proposed as a promising solution to structural variant calling. However, computational and technical limitations remain, especially in the context of population genetics where false positives and false negatives may alter allele frequencies. We explored the utility of HiFi PacBio reads to determine structural variants using 3 pre-existing tools and a BLAST comparison.

By looking at three programs designed to call structural variants, Minimap2, Pbsv, and Sniffles, we ascertained that these programs were not confirming our Illumina reads at a sufficient rate individually. Individual confirmation rates ranged from 3.2%-67.5% across individual bioinformatics pipelines. *Drosophila* is known to have many small structural variants in comparison with mammals. Deletions accumulate rapidly in *Drosophila*, creating gaps in alignment that make it more difficult to clarify mutation state. We find that complex variation is difficult for existing aligners to solve. To confirm our suspicions we used coverage data and investigated these complex regions where we frequently, and were able to find signs in the coverage that there was likely some kind of variation occurring, whether it be duplications, rearrangements, or other forms of variation.

Taking all of these factors into consideration, we aligned sequence data for these regions a BLAST against and the long-read data. Once we did this we were able to confirm rearrangements at a rate of 79.7%-87.2% from strain to strain S20. In aggregate across all 4 bioinformatic pipelines, we confirm 100% of rearrangement genotypes. BLAST is not designed to align long read sequence data, however with BLAST we are able to confirm a total of 100% that these regions do share similarity based on nucleotide identity and that the current tools commonly used to call these mutations are not accurately handling all cases of structural variation in *Drosophila*.

The prospects of structural variant calling in *Drosophila* with new HiFi sequence technology are promising. However, greater computational and bioinformatic analysis, likely with species-specific parameter tuning is likely necessary to solve these technical issues in data analysis for complex regions of the genome.

Table S1: Allele frequencies for highlighted UV genes (*Parp*, *Victoria*, *spel1*), "random" genes (*pnut*, *NUCB1*), and regions with no genes in the area.

Region/Ortholog	<i>D.san</i> freq	Mainland <i>D.yak</i> freq	Island <i>D.yak</i> freq
<i>Parp</i>	19/60	1/20	1/33
<i>spel1</i>	36/83	1/25	1/44
<i>Victoria</i>	26/72	1/20	1/37
<i>pnut</i>	15/73	1/26	0/41
<i>NUCB1</i>	28/82	26/27	37/38
2R:21138315-2L:4600409	40/86	0/27	0/27
X:11165668-X:7882823	23/66	0/19	2/38

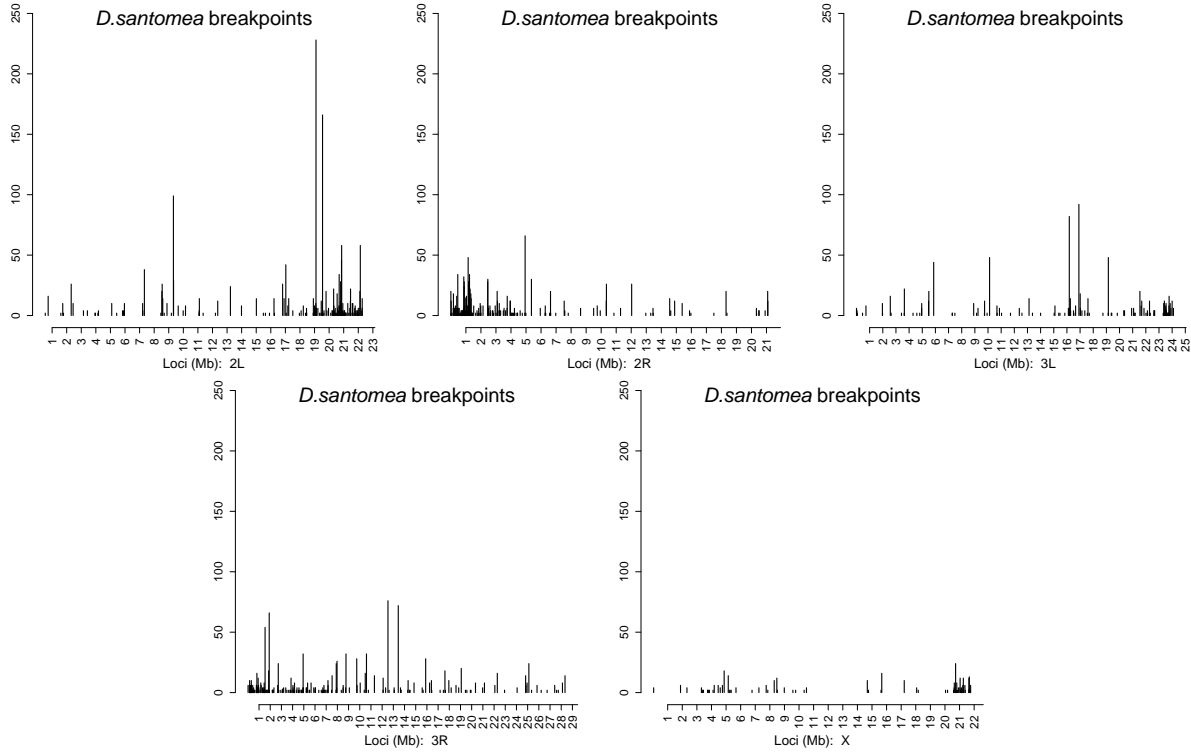


Figure S1: Number of rearrangement breakpoints in 10kb windows along each autosome and the X chromosome in *D. santomea*. Centromeres on chromosome 2, 3, and the X display hotspots, with a maximum of 250 rearrangements per window. Recombination suppression near the centromeres is expected to allow detrimental rearrangements to persist in populations, increasing rearrangement numbers.

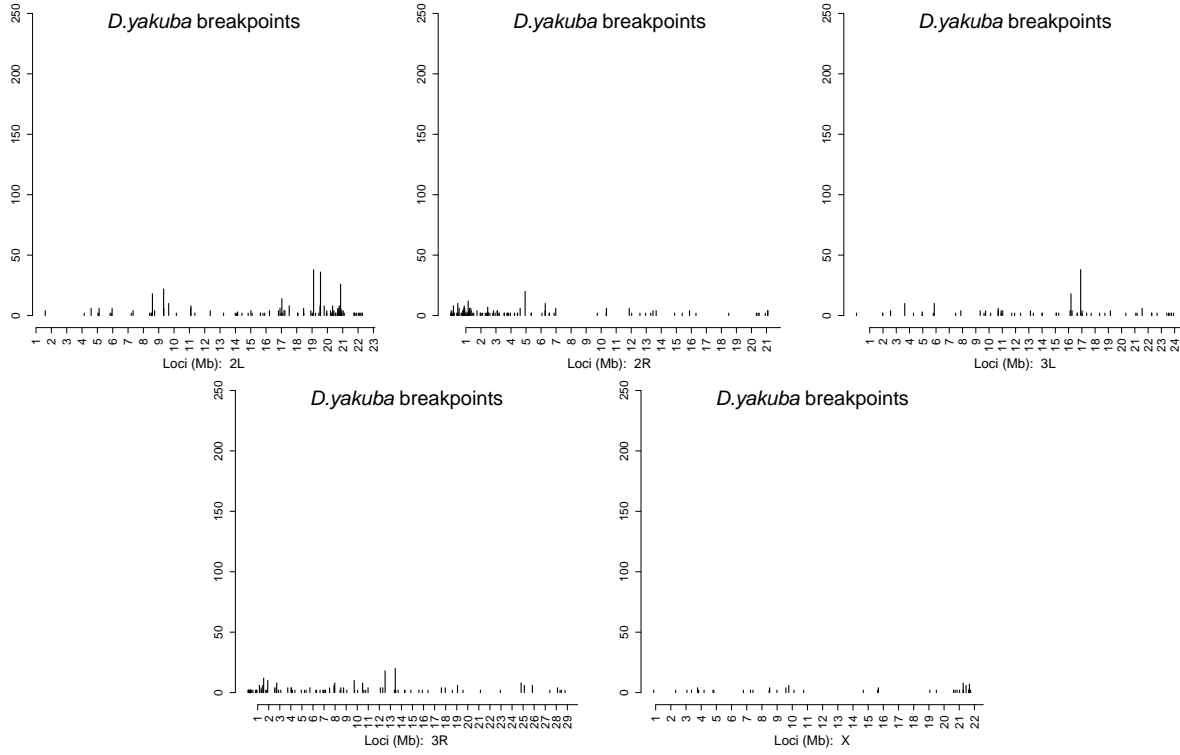


Figure S2: Number of rearrangement breakpoints in 10kb windows along each autosome and the X chromosome in *D. yakuba*. Centromeres on chromosome 2, 3, and the X display hotspots, with a maximum of 80 rearrangements per window, less dynamic than compared with more distantly related *D. santomea*.

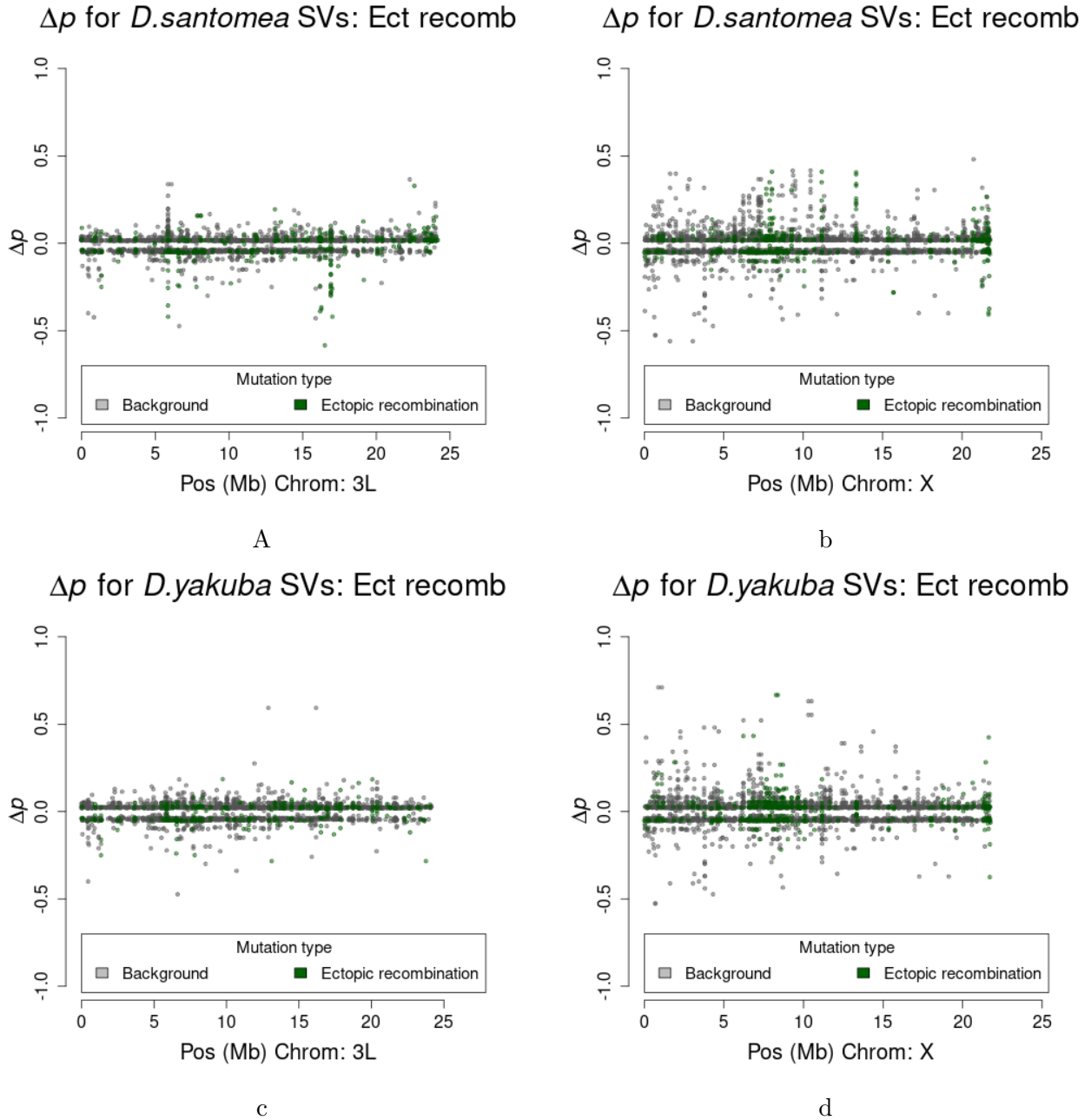


Figure S3: Population differentiation as shown via Δp A) Between *D. santomea* and mainland ancestral *D. yakuba* on autosome 3L. B) Between *D. santomea* and mainland ancestral *D. yakuba* on the X chromosome C) Between Island *D. yakuba* and ancestral mainland *D. yakuba* on the autosome 3L. D) Between Island *D. yakuba* and ancestral mainland *D. yakuba* on the X chromosome. The x-axis shows genomic position on the chromosome in megabases, and the y-axis is difference in allele frequencies between the test population and the mainland. Points in dark green highlight the rearrangements associated with facilitating ectopic recombination. We observe greater levels of differentiation on the X compared to the autosomes in both populations.

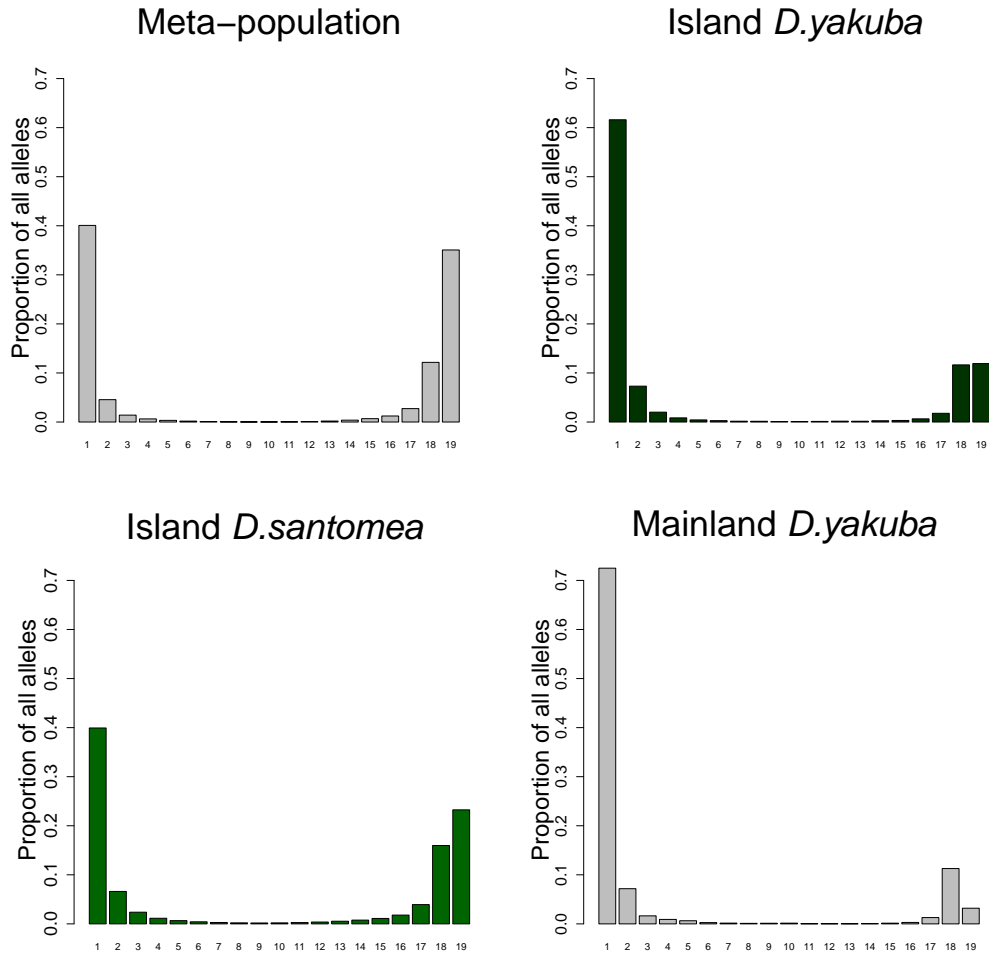


Figure S4: Site frequency spectrum once only rearrangements associated with TEs are selected A) Site frequency spectrum of the meta-population of the study. Polarized ancestral state with *D. teissieri* and projected down to $n=19$ using the geometric distribution. The increase in high frequency variants is represented in only some of the sub-populations once they are separated. B) Site frequency spectrum of *D. santomea*. Polarized ancestral state with *D. teissieri* and projected down to $n=19$ using the geometric distribution. The increase in high frequency variants is much greater than that of the mainland *D. yakuba* C) Site frequency spectrum of the island *D. yakuba*. Polarized ancestral state with *D. teissieri* and projected down to $n=19$ using the geometric distribution. The increase in high frequency variants is slightly greater than that of the mainland *D. yakuba*, but not as much as *D. santomea*, likely related to divergence time D) Site frequency spectrum of mainland *D. yakuba*. Polarized ancestral state with *D. teissieri* and projected down to $n=19$ using the hypergeometric distribution. Lacks the increase in high frequency variants that is present in both of the other sub-populations

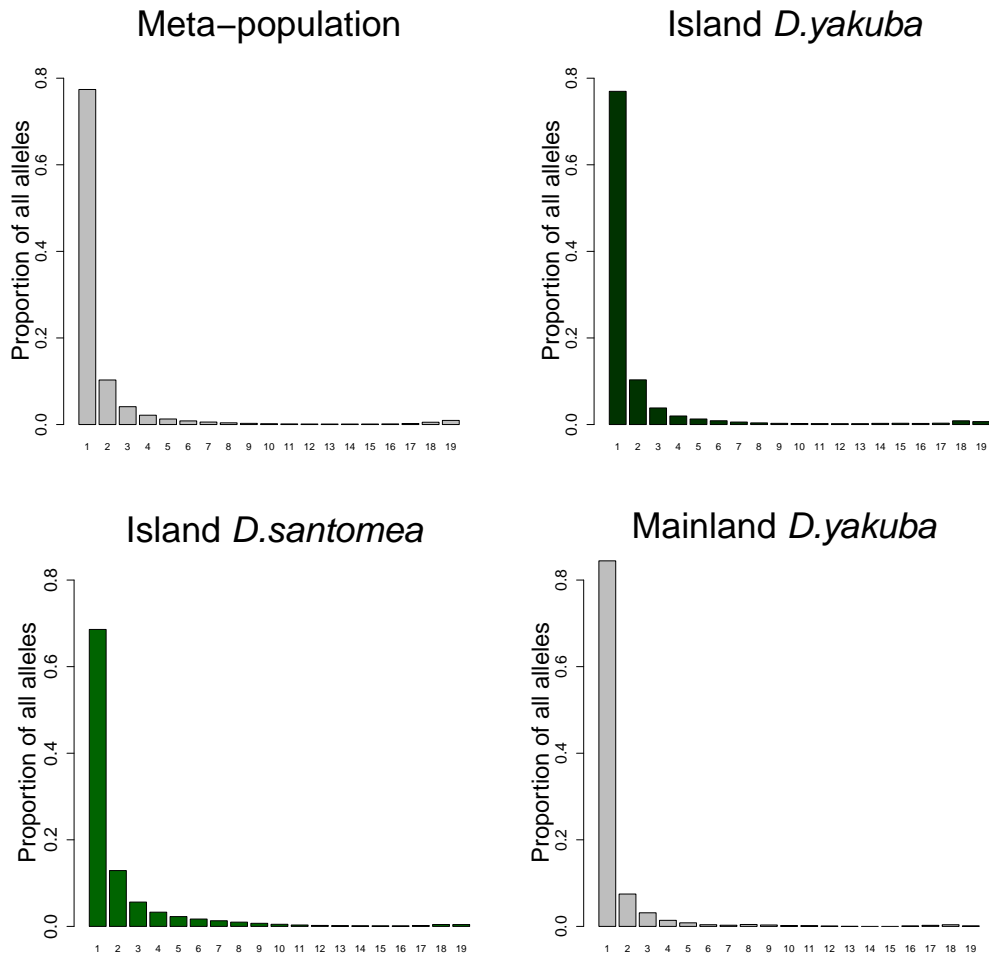


Figure S5: Site frequency spectrum once only rearrangements associated with TEs are removed A) Site frequency spectrum of the meta-population of the study. Polarized ancestral state with *D. teissieri* and projected down to $n=19$ using the geometric distribution. The increase in high frequency variants is represented is missing from all populations. B) Site frequency spectrum of *D. santomea*. Polarized ancestral state with *D. teissieri* and projected down to $n=19$ using the geometric distribution. The increase in high frequency variants is lost once TEs are removed. C) Site frequency spectrum of the island *D. yakuba*. Polarized ancestral state with *D. teissieri* and projected down to $n=19$ using the geometric distribution. The increase in high frequency variants is lost once TEs are removed. D) Site frequency spectrum of mainland *D. yakuba*. Polarized ancestral state with *D. teissieri* and projected down to $n=19$ using the hypergeometric distribution. The increase in high frequency variants is lost once TEs are removed.

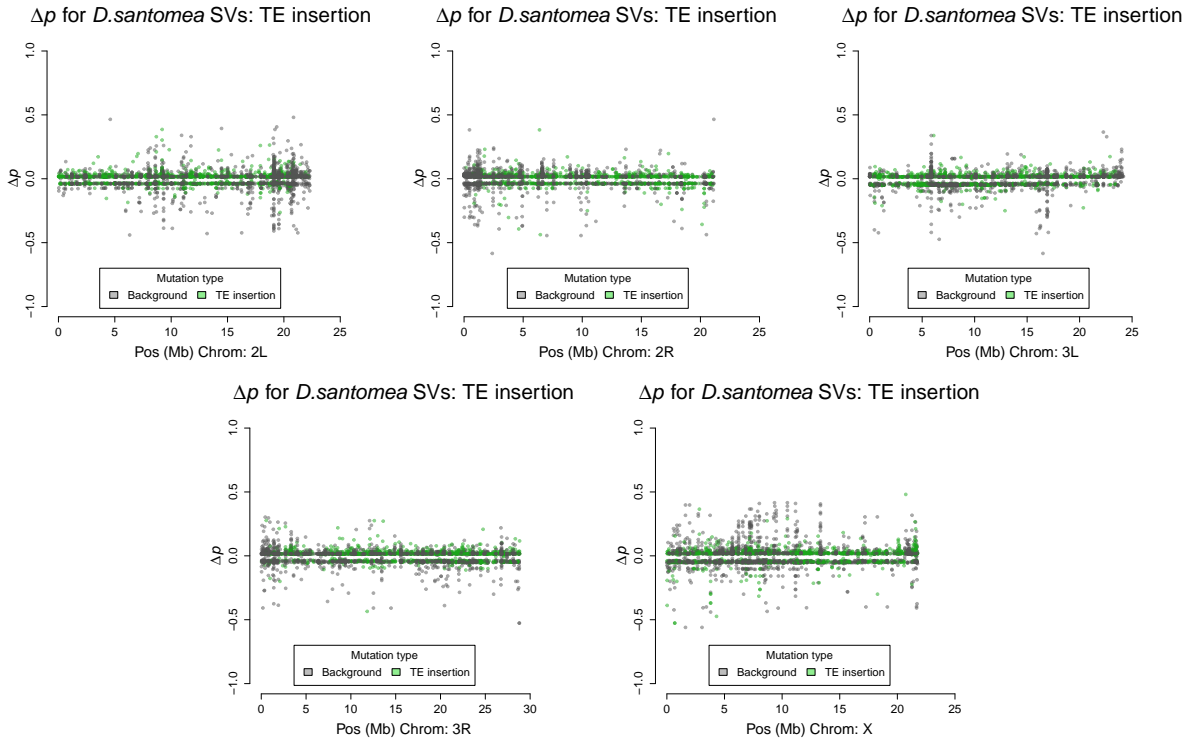


Figure S6: Population differentiation as shown via Δp A) Between *D. santomea* and mainland ancestral *D. yakuba* on autosome 3L. B) Between *D. santomea* and mainland ancestral *D. yakuba* on the X chromosome C) Between Island *D. yakuba* and ancestral mainland *D. yakuba* on the autosome 3L. D) Between Island *D. yakuba* and ancestral mainland *D. yakuba* on the X chromosome. The x-axis shows genomic position on the chromosome in megabases, and the y-axis is difference in allele frequencies between the test population and the mainland. Points in dark green highlight the rearrangements associated with TE insertions. We observe greater levels of differentiation on the X compared to the autosomes in both populations.

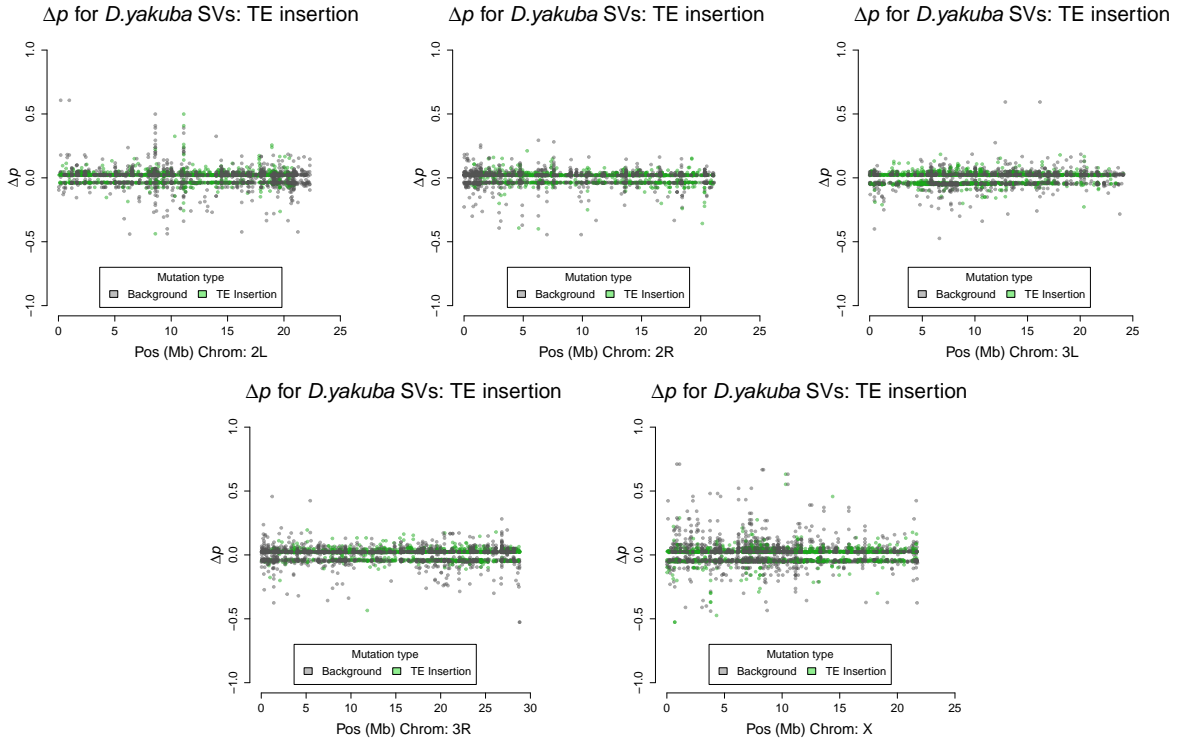


Figure S7: Population differentiation as shown via Δp A) Between island *D. yakuba* and mainland ancestral *D. yakuba* on autosome 3L. B) Between *D. santomea* and mainland ancestral *D. yakuba* on the X chromosome C) Between Island *D. yakuba* and ancestral mainland *D. yakuba* on the autosome 3L. D) Between Island *D. yakuba* and ancestral mainland *D. yakuba* on the X chromosome. The x-axis shows genomic position on the chromosome in megabases, and the y-axis is difference in allele frequencies between the test population and the mainland. Points in dark green highlight the rearrangements associated with TE insertions. We observe greater levels of differentiation on the X compared to the autosomes in both populations.

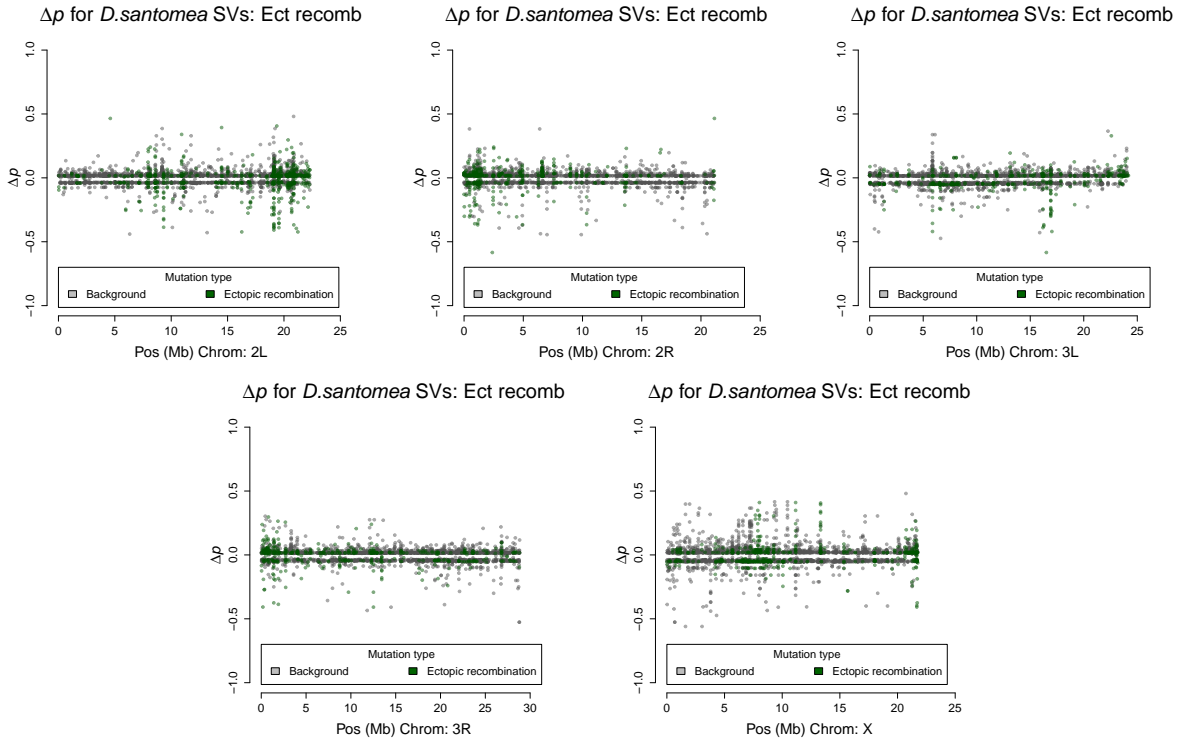


Figure S8: Population differentiation as shown via Δp A) Between *D. santomea* and mainland ancestral *D. yakuba* on autosome 3L. B) Between *D. santomea* and mainland ancestral *D. yakuba* on the X chromosome C) Between Island *D. yakuba* and ancestral mainland *D. yakuba* on the autosome 3L. D) Between Island *D. yakuba* and ancestral mainland *D. yakuba* on the X chromosome. The x-axis shows genomic position on the chromosome in megabases, and the y-axis is difference in allele frequencies between the test population and the mainland. Points in dark green highlight the rearrangements associated with facilitating ectopic recombination. We observe greater levels of differentiation on the X compared to the autosomes in both populations.

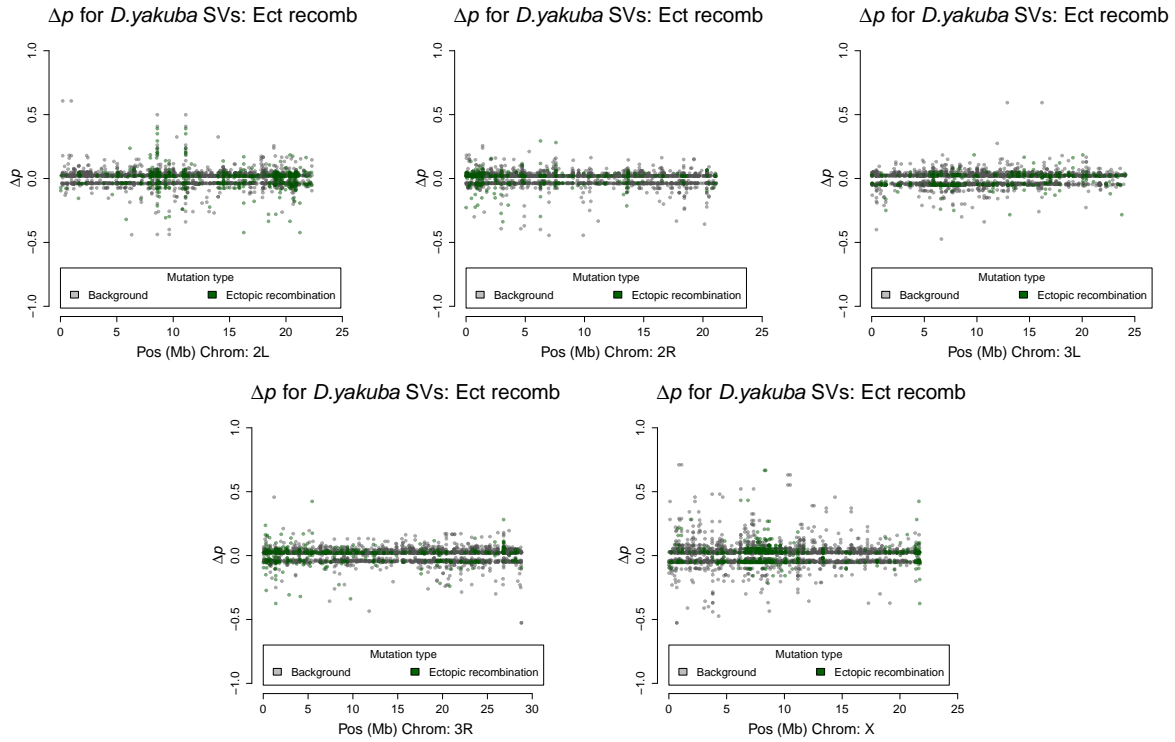


Figure S9: Population differentiation as shown via Δp A) Between island *D. yakuba* and mainland ancestral *D. yakuba* on autosome 3L. B) Between *D. santomea* and mainland ancestral *D. yakuba* on the X chromosome C) Between Island *D. yakuba* and ancestral mainland *D. yakuba* on the autosome 3L. D) Between Island *D. yakuba* and ancestral mainland *D. yakuba* on the X chromosome. The x-axis shows genomic position on the chromosome in megabases, and the y-axis is difference in allele frequencies between the test population and the mainland. Points in dark green highlight the rearrangements associated with facilitating ectopic recombination. We observe greater levels of differentiation on the X compared to the autosomes in both populations.

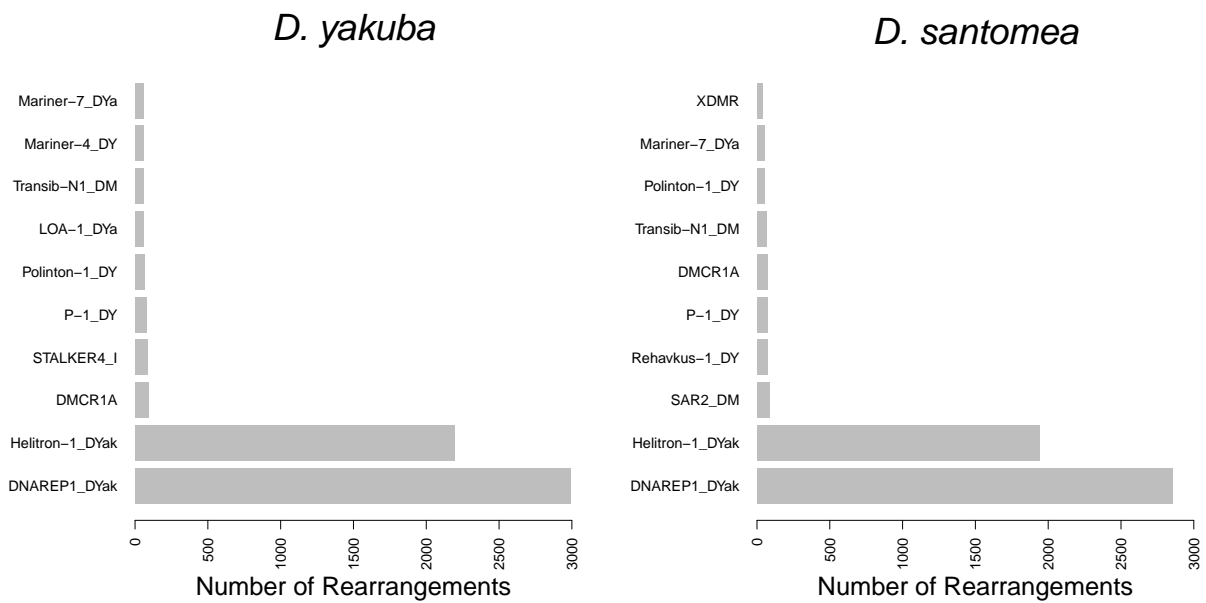


Figure S10: Number of rearrangements matching TE families for an entire subpopulation A) *D. santomea* and B) *D. yakuba*. The most common rearrangements come from *DNAREP1* and *Helitrons* in both species.

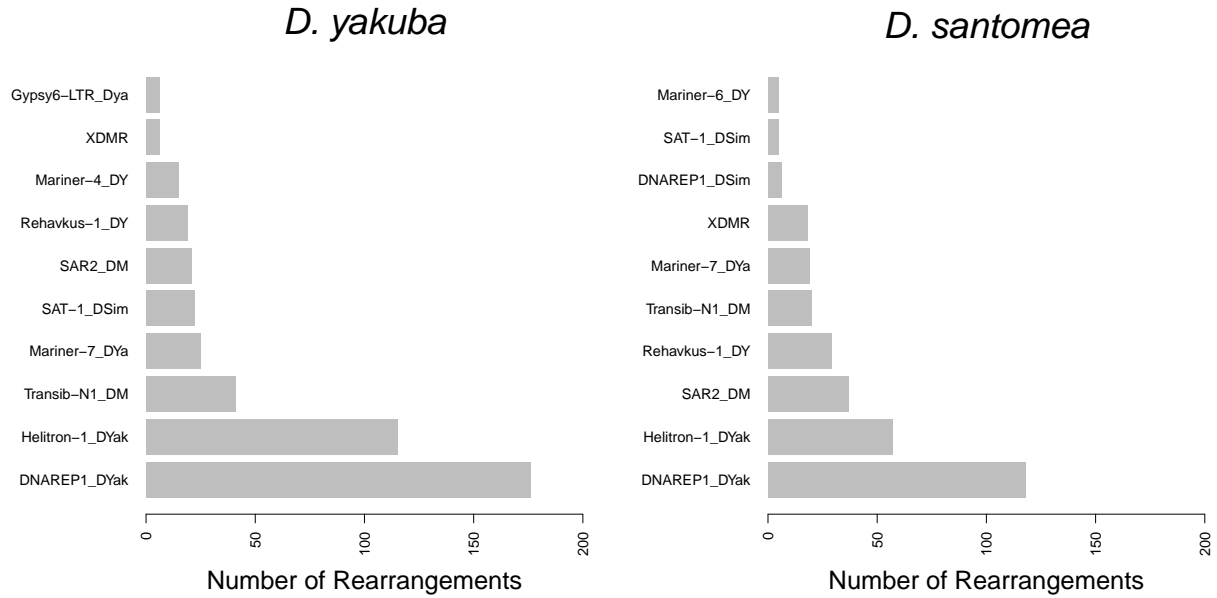


Figure S11: Number of rearrangements matching TE families associated with strong differentiation in A) *D. santomea* and B) *D. yakuba*. The most common rearrangements come from *DNAREP1* and *Helitrons* in both species but minor elements constitute a greater proportion compared with background incidence rates.

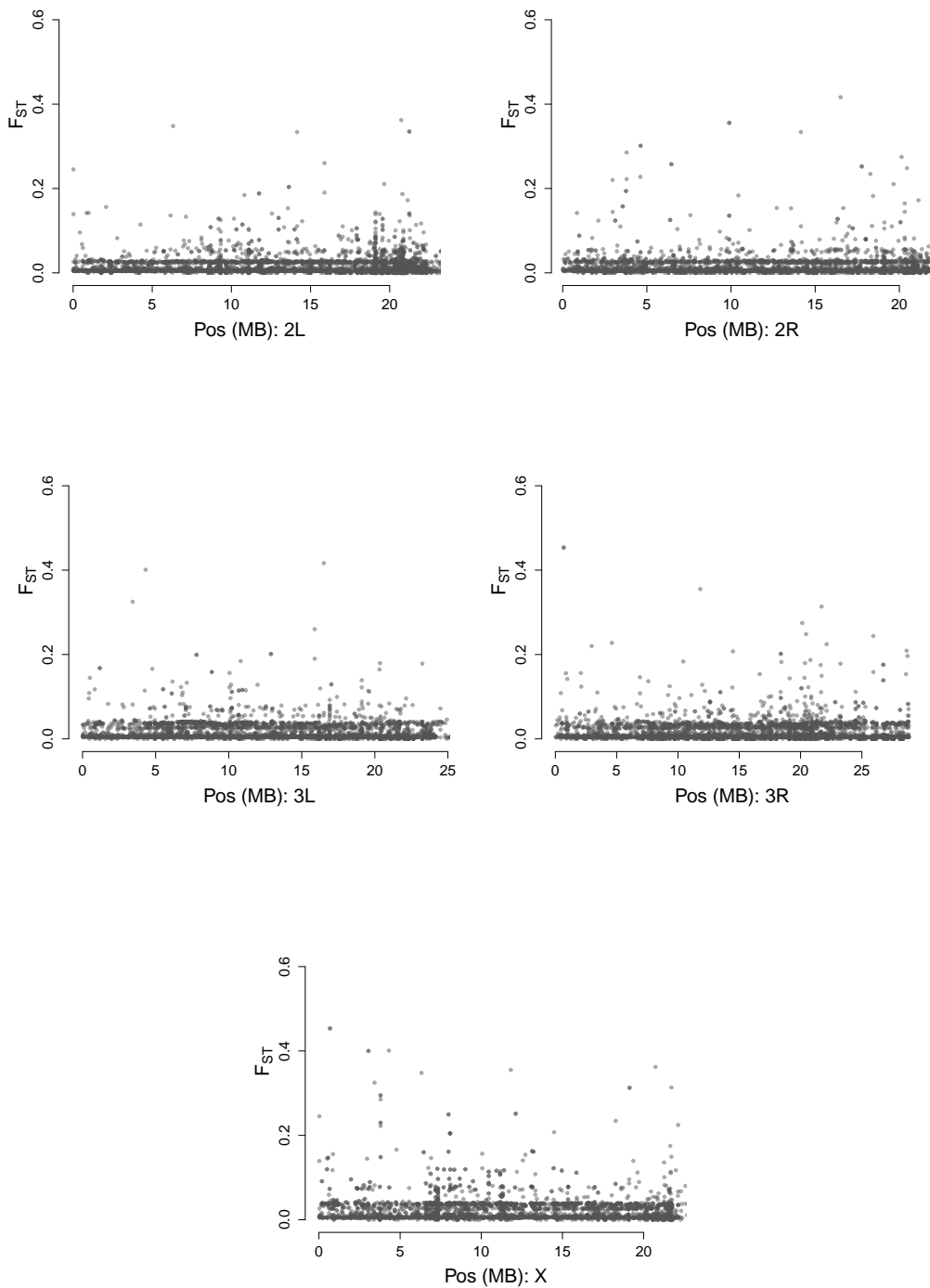


Figure S12: F_{ST} along the autosomes and the X chromosome shows high rates of population differentiation on the X and autosomes in *D. santomea* compared with the ancestral mainland population of *D. yakuba*. Most variation shows minimal divergence, with peaks associated with genome outliers. This complementary measure of differentiation to Δp also shows that structural variation is associated with population divergence on the island of São Tomè.

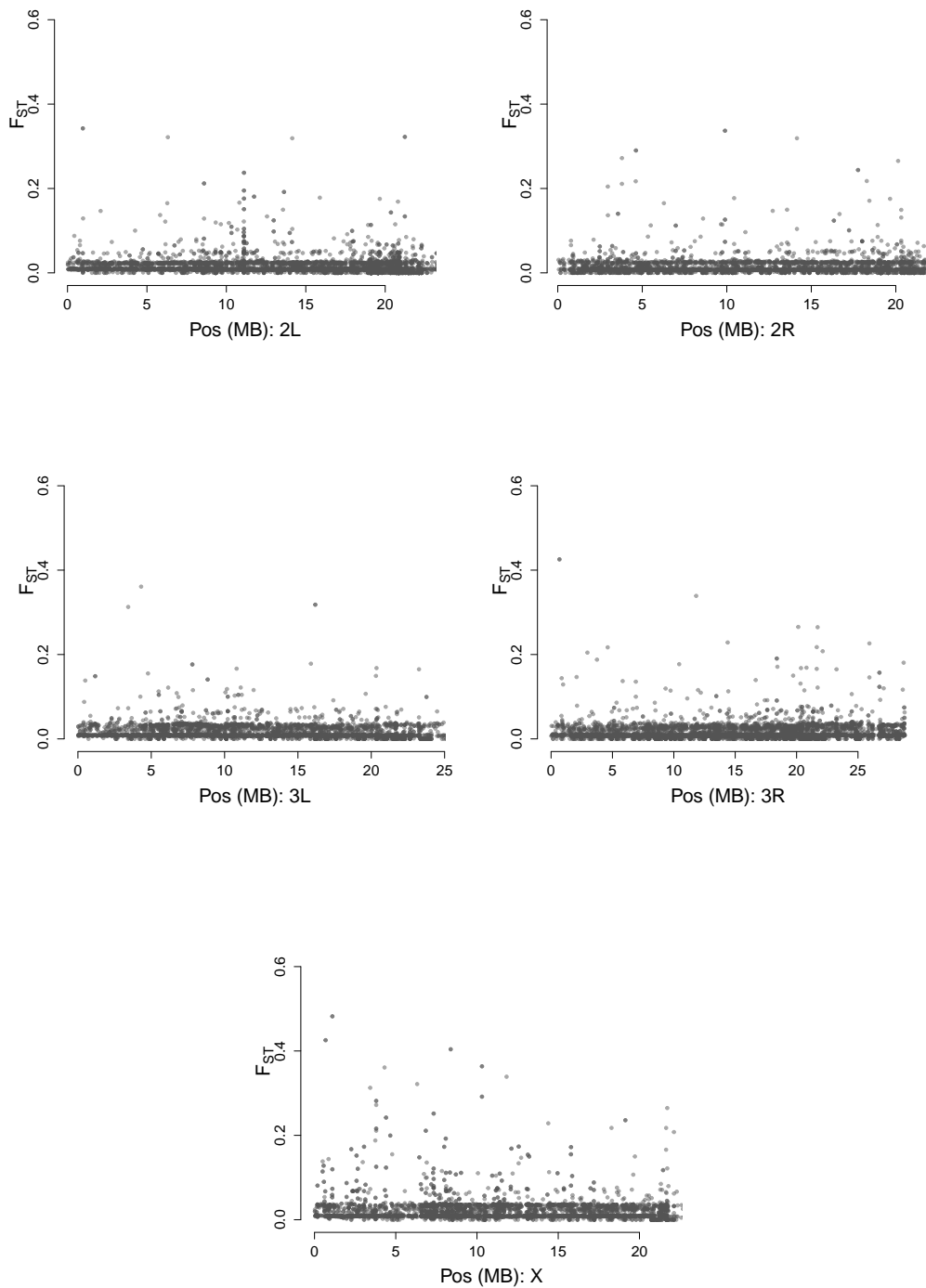


Figure S13: F_{ST} along the autosomes and the X chromosome shows high rates of population differentiation on the X and autosomes in island *D. yakuba* compared with the ancestral mainland population. Most variation shows minimal divergence, with peaks associated with genome outliers. This complementary measure of differentiation to Δp also shows that structural variation is associated with population divergence on the island of São Tomè.

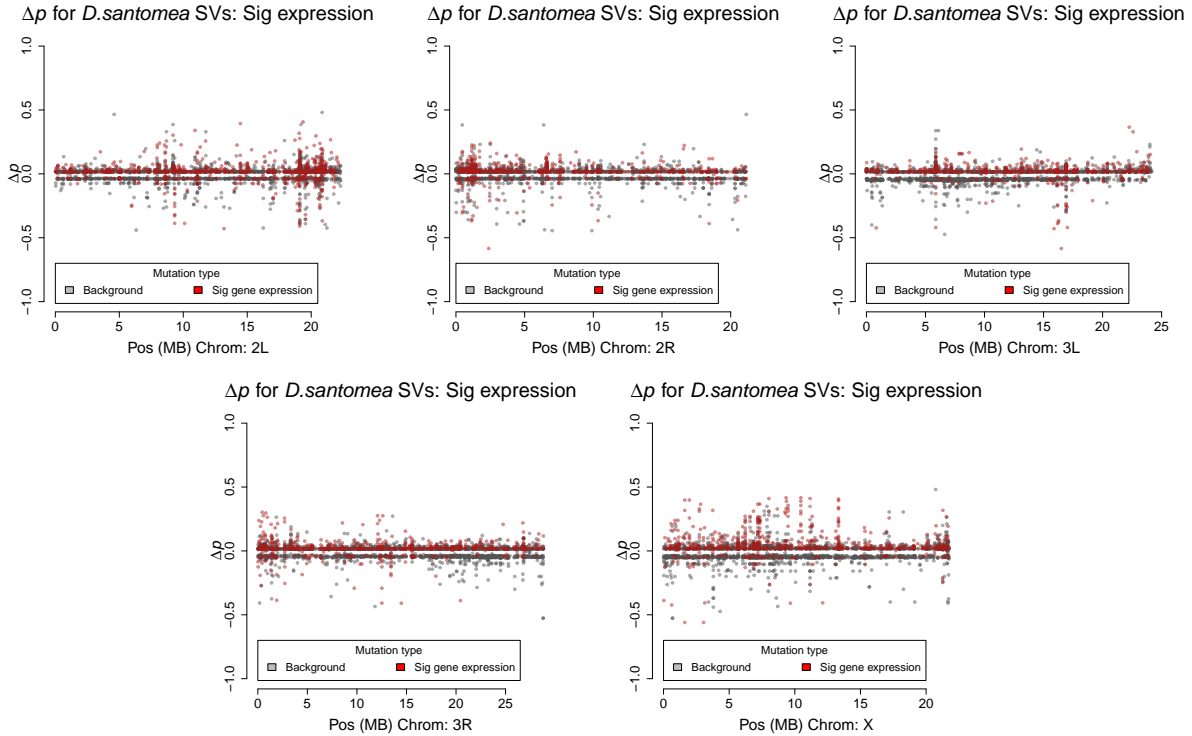


Figure S14: Population differentiation as shown via Δp A) Between *D. santomea* and mainland ancestral *D. yakuba* on autosome 3L. B) Between *D. santomea* and mainland ancestral *D. yakuba* on the X chromosome C) Between Island *D. yakuba* and ancestral mainland *D. yakuba* on the autosome 3L. D) Between Island *D. yakuba* and ancestral mainland *D. yakuba* on the X chromosome. The x-axis shows genomic position on the chromosome in megabases, and the y-axis is difference in allele frequencies between the test population and the mainland. Points in red highlight the rearrangements associated with significant gene expression. We observe greater levels of differentiation on the X compared to the autosomes in both populations and rearrangements associated with significant expression changes on the X show strong differentiation. These results suggest that gene expression changes induced by rearrangements are important for local adaptation.

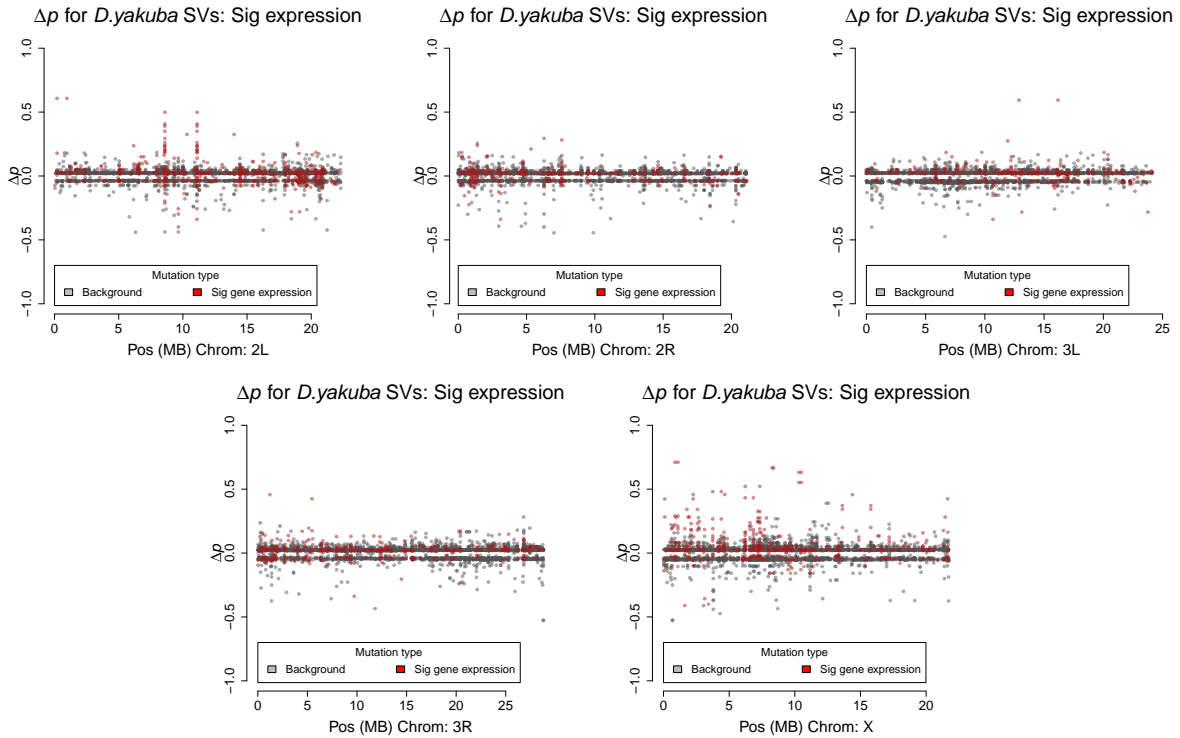


Figure S15: Population differentiation as shown via Δp A) Between the island *D. yakuba* and mainland ancestral *D. yakuba* on autosome 3L. B) Between *D. santomea* and mainland ancestral *D. yakuba* on the X chromosome C) Between Island *D. yakuba* and ancestral mainland *D. yakuba* on the autosome 3L. D) Between Island *D. yakuba* and ancestral mainland *D. yakuba* on the X chromosome. The x-axis shows genomic position on the chromosome in megabases, and the y-axis is difference in allele frequencies between the test population and the mainland. Points in red highlight the rearrangements associated with significant gene expression. We observe greater levels of differentiation on the X compared to the autosomes in both populations and rearrangements associated with significant expression changes on the X show strong differentiation. These results suggest that gene expression changes induced by rearrangements are important for local adaptation.

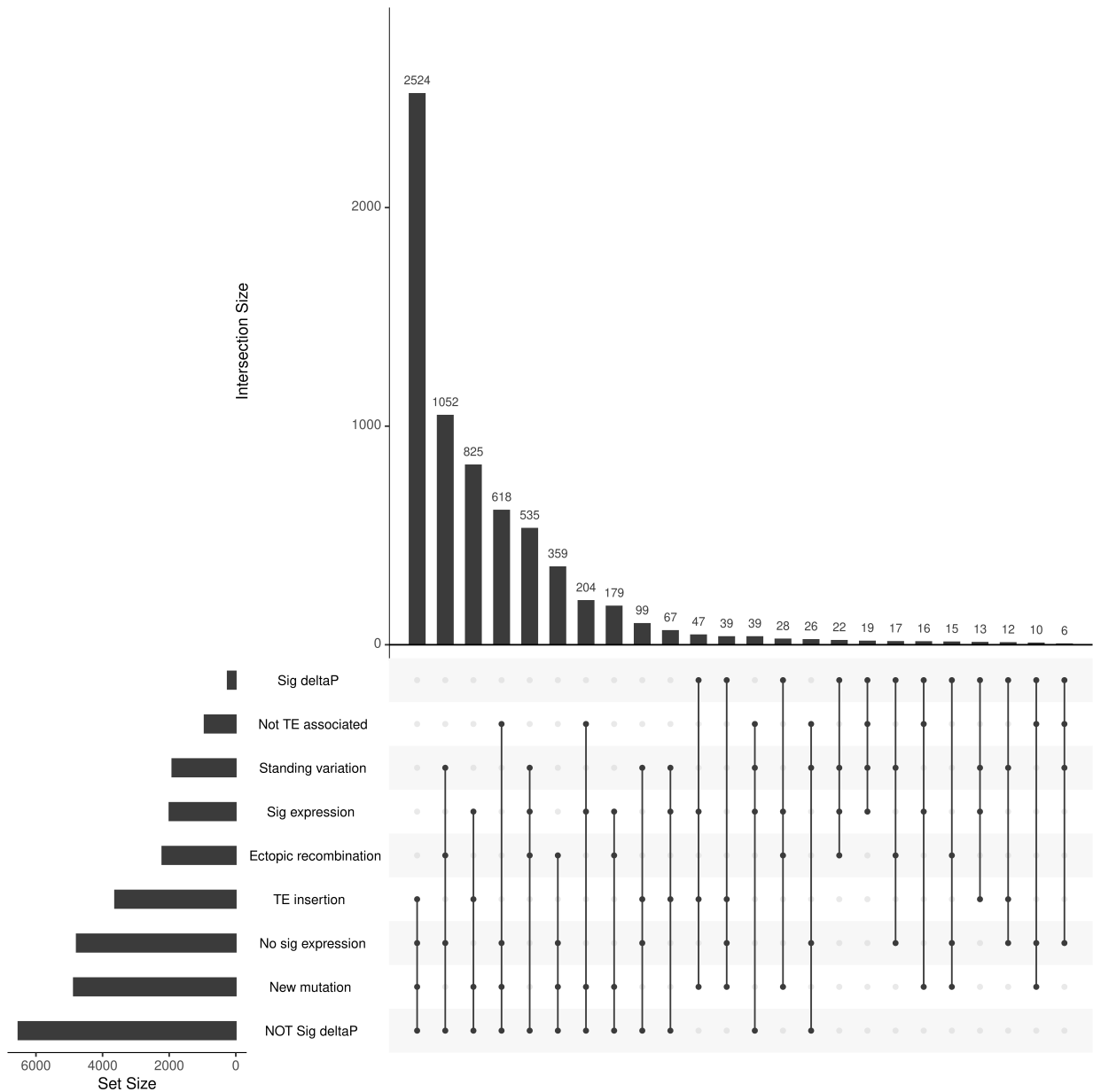


Figure S16: Upset plot showing factors associated with rearrangements. Novel TE insertions without population differentiation and without changes in gene expression are the most common type of mutation in *D. santomea*. New mutations induced by TE insertion with significant changes in gene expression are the most common type of variation that contributes to population differentiation.

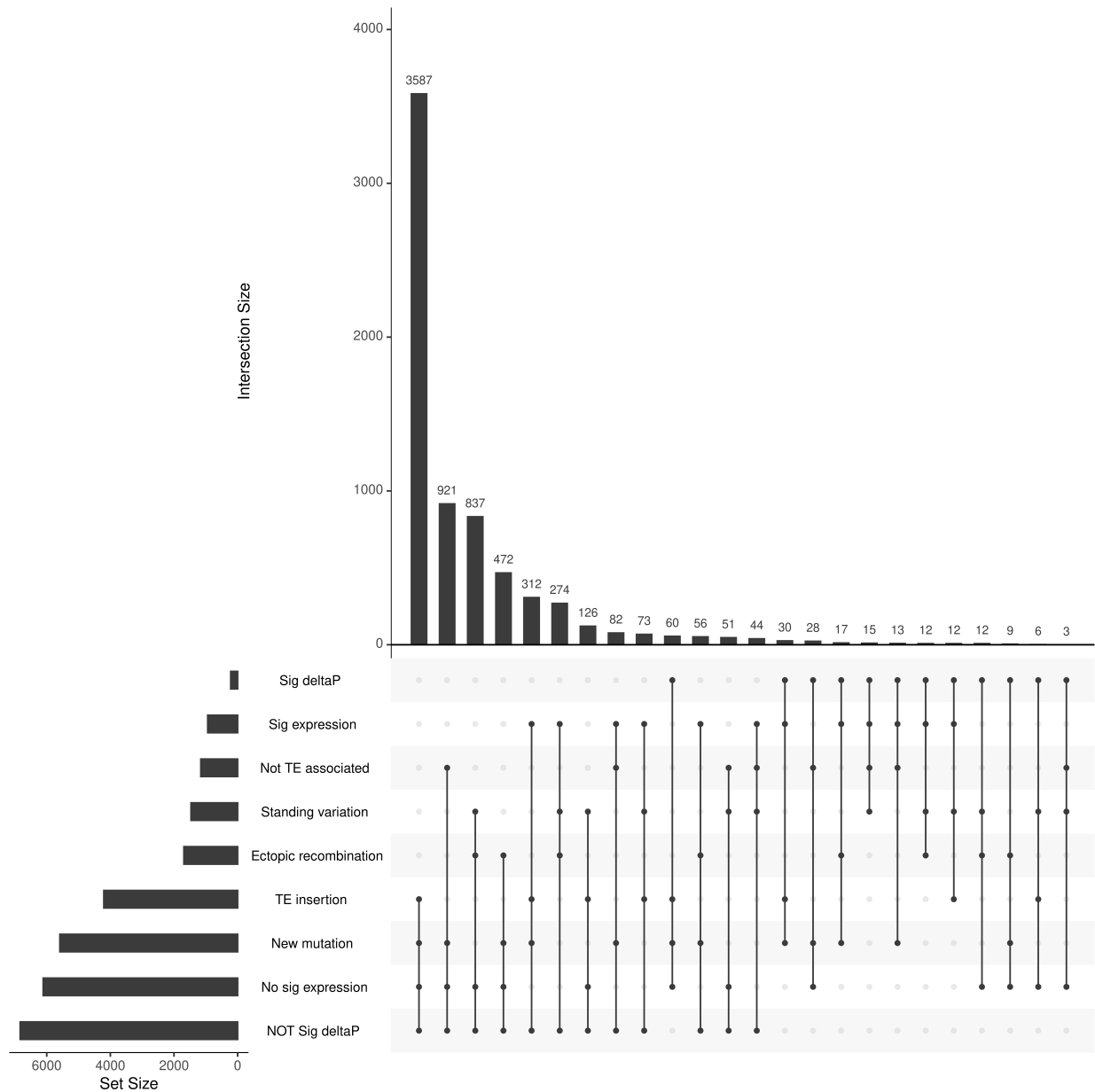
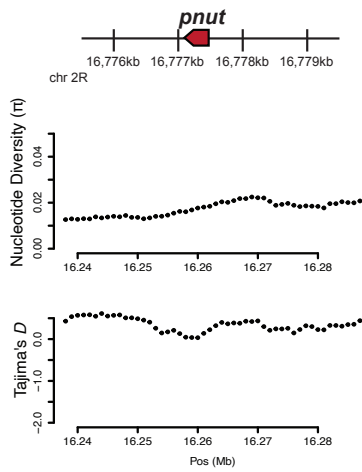


Figure S17: Upset plot showing factors associated with rearrangements. Novel TE insertions without population differentiation and without changes in gene expression are the most common type of mutation in *D. yakuba*. New mutations induced by TE insertion with significant changes in gene expression are the most common type of variation that contributes to population differentiation.

A. 2L_1678226_1678265_3R_3348038_3348386

- 15/73 Island *D. santomea*
- 1/26 Mainland *D. yakuba*
- 0/41 Island *D. yakuba*



B. 2L_19108464_19108655_3L_16266875_16267219

- 28/82 Island *D. santomea*
- 26/27 Mainland *D. yakuba*
- 37/38 Island *D. yakuba*

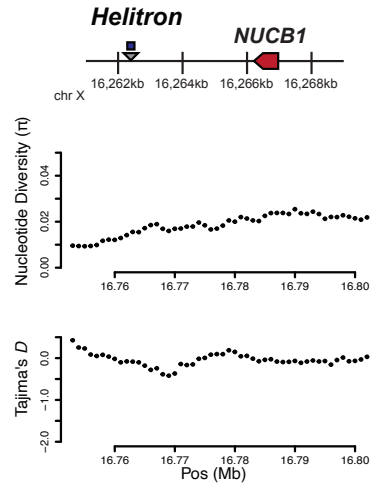


Figure S18: Two regions associated with chromosomal rearrangements that show significant changes in both population differentiation and signatures of selection and are within 5kb of genes A) A rearrangement near the ortholog to a cell organization gene *pnut*, and slight shows drops in π and Tajima's (D) (local minima $\pi=0.00966$ and $D=-0.421$). B) A rearrangement mediated by a *SAT* element, and shows minute drops in π and Tajima's (D) (local minima $\pi=0.0141$ and $D=-0.034$). This rearrangement is heavily present in the *D. yakuba* populations. Genomic averages for π and Tajima's D are $\pi=0.0159$ and $D=-0.0445$

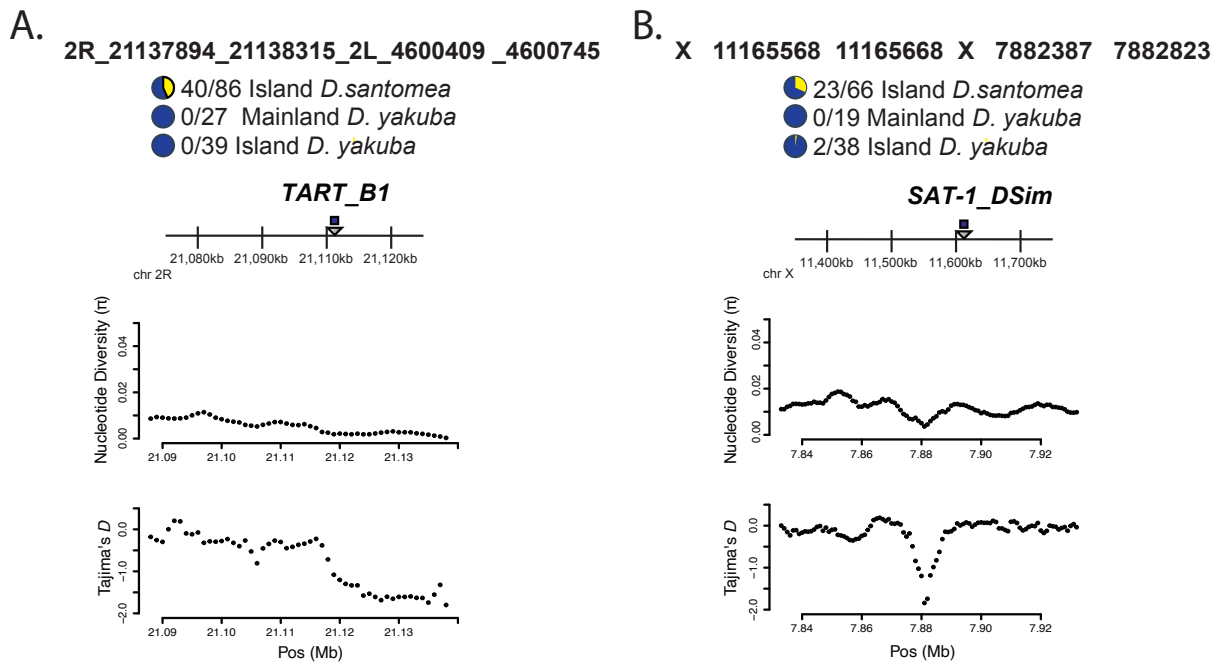


Figure S19: Two regions associated with chromosomal rearrangements that show significant changes in both population differentiation and signatures of selection A) A rearrangement mediated by a *TART-B1* element that is only present in *D. santomea*, and shows drops in π and Tajima's (D) (local minima $\pi=0.000111$ and $D=-1.80$). B) A rearrangement mediated by a *SAT-1* element, and shows drops in π and Tajima's (D) (local minima $\pi=0.00176$ and $D=-1.84$). Genomic averages for π and Tajima's D are $\pi=0.0159$ and $D=-0.0445$

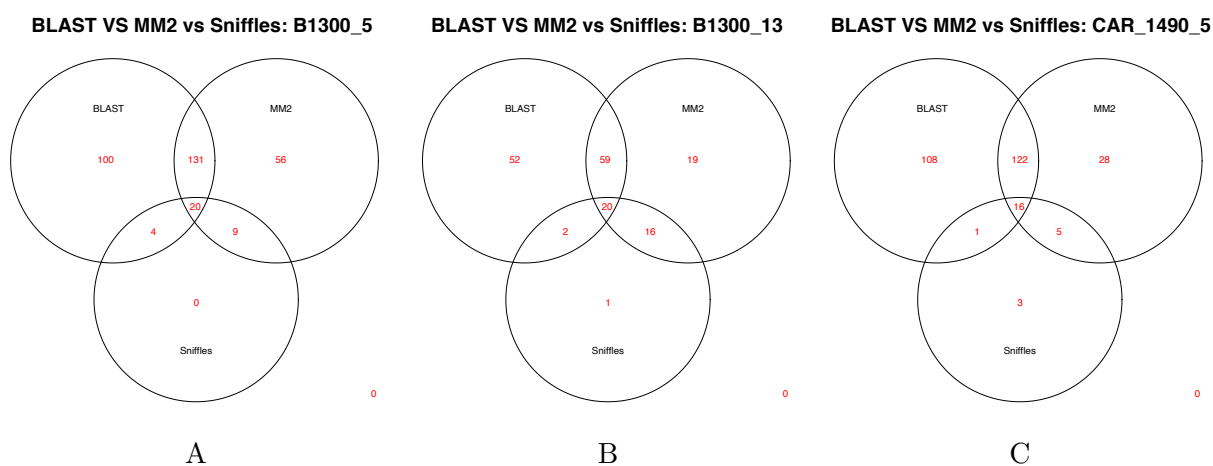


Figure S20: Confirmation rates for 336 rearrangements in three strains with PacBio HiFi data. We observe low confirmation rates from Sniffles, which is tuned to identify large rearrangements common in mammals. Minimapp2 alignments confirm a moderate number of rearrangements in each strain. Using BLAST to search for reads matching to rearrangement breakpoints, we are able to confirm an additional 308 rearrangements. These differing rates of confirmation suggest that greater methods development is required to identify moderately sized rearrangement sequences in long read data.